A STUDY OF THE CATALYTIC CONVERSION OF SYNTHESIS GAS
TO LOW-MOLECULAR-WEIGHT HYDROCARBONS

A Thesis

by

TING YEE CHAN

Submitted to the Graduate College of

Texas A&M University

in partial fulfillment of the requirement for the degree of

MASTER OF SCIENCE
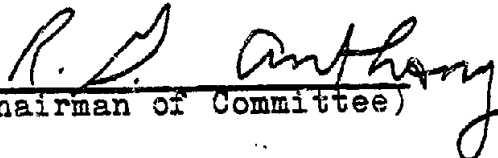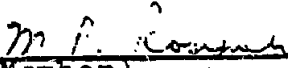
August 1981

Major Subject: Chemical Engineering

A STUDY OF CATALYTIC CONVERSION OF SYNTHESIS GAS

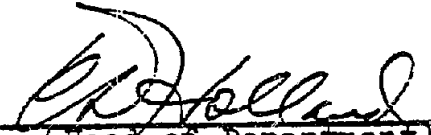TO LOW MOLECULAR WEIGHT HYDROCARBONS

A Thesis

by

TING YEE CHAN

Approved as to style and content by

_____
(Chairman of Committee)

_____   _____
(Member)   (Member)

_____   _____
(Member)   (Head of Department)

August 1981

ii

p

ABSTRACT

A Study of Catalytic Conversion of Synthesis Gas
to Low Molecular Weight Hydrocarbons (August 1981)

Ting Yee Chan,   B.S., M.I.T.

Chairman of Advisory Committee: Dr. R. G. Anthony

The search for alternative sources of energy has
provided the stage for the examination of catalytic
reactions which can influence the supply of low molecular
weight chemical feedstocks, such as ethylene, propylene, and
butadiene. Synthesis gas produced from partial oxidation of
coal is considered the basic building block for all
alternative chemical feedstock synthesis. However, the
classical Fischer-Tropsch synthesis catalysts exhibit poor
selectivity toward low molecular weight hydrocarbons.
Utilizing non-trival bifunctional catalysts which can
catalyze methanol synthesis and methanol decomposition to
hydrocarbons, synthesis gas was converted to hydrocarbons
with selectivity of 100% for C_1 to C_4 at reaction
temperatures of 595 to 731 K and pressures from 27 to 68
atm..

Zinc oxide and copper oxide were used to promote the
methanol synthesis, and the acidic-ion exchanged form of
erionite was used to catalyze the subsequent methanol
decomposition to hydrocarbons. Catalyst preparation

techniques used were physical mixture, impregnation, and co-precipitation. Identification and characterization of catalysts, before and after the reaction, were accomplished by powder X-ray diffraction, using $Cu-K_\alpha$ radiation.

Methanol and/or dimethylether which are the precursors for hydrocarbons were found in the reactor exit. The hydrocarbons produced were between C_1 and C_4 which demonstrate the shape selectivity of erionite. The olefinic content of the hydrocarbon produced was small compared to the paraffinic content. Experiments with ethylene and hydrogen indicated that the methanol synthesis component of the hybrid catalyst was highly active toward olefin hydrogenation. Addition of water into the feed of ethylene and hydrogen caused a substantial reduction of ethylene hydrogenation. The water gas shift reaction, catalyzed by methanol synthesis component, was observed to be in dynamic equilibrium.

Comparison of the different catalysts showed that erionite impregnated with zinc oxide had the highest selectivity and activity toward paraffins and olefins.

ACKNOWLEDGEMENTS

Dedicated

to

My Nan

TABLE OF CONTENTS

p

p

LIST OF FIGURES

p

LIST OF TABLES

CHAPTER I

INTRODUCTION

The unplesant reality of the energy crisis has
stimulated the resurgence of the search for alternative
chemical feedstock sources. There are many potential
sources such as tar sand, shale oil, biomass, and coal.
Among this group of potential sources, coal has received the
most attention because of its abundance and the existence of
mining technology. Presently, gasification is one of the
generally accepted strategies to utilize coal as the carbon
source for chemical feedstock. Several coal gasification
processes have been demonstrated commercially to be
economically and technically viable. The major product of
coal gasification is a mixture of carbon monoxide and
hydrogen, commonly called synthesis gas.

Synthesis gas produced from partial oxidation of coal
is considered the basic building block for all alternative
chemical feedstock synthesis. Conversion of synthesis gas
to chemical feedstock is not new in that the Germans were
producing fuel from synthesis gas during World War II. The
process that was used was the Fischer-Tropsch Synthesis

This thesis is presented in the style and format
of the AIChE Journal.

in which gaseous fuel, liquid fuel, and chemical feedstock were produced. The limiting factor in the utilization of synthesis gas by the Fischer-Tropsch Synthesis process was the non-selective nature of the products.

Consequently, numerous studies have been conducted to improve the selectivity of the Fischer-Tropsch process. Through these efforts, new avenues were opened for non-Fischer-Tropsch type hydrocarbon synthesis with higher selectivity. Of this type of non-Fischer-Tropsch Synthesis, methanol derived from synthesis gas has received much attention as the raw material for hydrocarbon synthesis, because the technology and economics of methanol production are well established. Many potential reaction pathways for methanol conversion to hydrocarbons were explored. Chang, et al. (1979) reported the catalytic conversion of methanol over a shape-selective catalyst to gasoline range hydrocarbons. Conversion of methanol to light olefins and paraffins were conducted by Lin, et al. (1978) and Singh (1980). However, limited attention was given to the selective conversion of synthesis gas to light olefins and paraffins by using methanol as the intermediate product.

The major objective of this thesis work has been to study a set of non-trival bifunctional catalysts which can selectively catalyze methanol synthesis and methanol decomposition to low molecular weight hydrocarbons. Zinc oxide and copper oxide were used to promote the methanol

synthesis, and the acidic-ion exchanged form of erionite was used to catalyze the subsequent methanol decomposition to hydrocarbons. Catalysts were prepared by physically mixing, by impregnation, and by co-precipitation. Identification and characterization of catalysts, before and after the reaction, were accomplished by powder X-ray diffraction, using Cu-K_α radiation.

The prepared catalysts were tested using a Berty reactor at temperatures of 595 to 731 K and pressures of 27 to 68 atm.. Quantitative analysis of the reaction effluent was obtained by gas chromatography. Activity and selectivity data were calculated from the material balances, and comparisons were made to determine the merits of each catalyst and preparation technique.

CHAPTER II

LITERATURE REVIEW

Hydrocarbon synthesis from synthesis gas has a long and extensive history. In conjunction with the recent methanol technology, it was within the interests of this work to filter the vast amount of information and to obtain the relative merits of each process.

Fischer-Tropsch Technology

The first catalytic synthesis gas conversion to liquid hydrocarbon study was reported by Badische Anilin und and Soda-Fabrik (1913) in Germany. In 1925 Fischer and Tropsch (Baird, et al.) developed the first commercial process. During World War II the German Fischer-Tropsch plants were producing six million barrels of gasoline, diesel oil, lubricating oil, and paraffin wax per year. The new discoveries of oil in the U.S. and in the Middle East following World War II have lowered interests in Fischer-Tropsch Synthesis until the recent energy crisis. The only commercial Fischer-Tropsch plant that exists today is South Africa's Sasol project.

The most often used catalyst in Fischer-Tropsch Synthesis was the promoted iron catalyst. Various reducible metal oxides and alkali metals were used as structural and electronic promoters, respectively. The products were hydrocarbons and oxygenates of various chain length. Only

methyl branching was observed, and there was no quarternary carbon in the product. The reaction mechanism was proposed to be the oligomerization of synthesis gas. The overall reaction can be represented as:

Paraffin Formation

$$(2n+1)H_2 + nCO \longrightarrow C_2H_{2n+2} + nH_2O \qquad (1)$$

Olefin Formation

$$2mH_2 + mCO \longrightarrow C_mH_{2m} + mH_2O \qquad (2)$$

Oxygenate Formation

$$2xH_2 + xCO \longrightarrow C_xH_{2x+1}OH + (x+1)H_2 \qquad (3)$$

Water Gas Shift

$$yCO + yH_2O \longrightarrow yCO_2 + yH_2 \qquad (4)$$
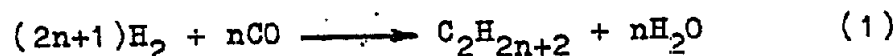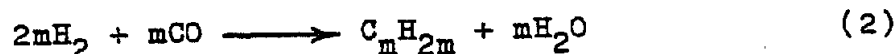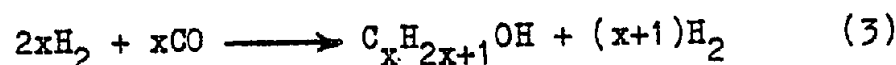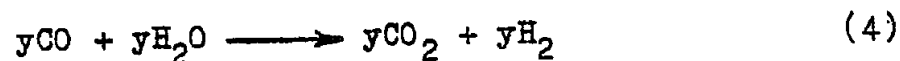
Thermodynamic considerations revealed that the hydrocarbon and oxygenate formation were highly favorable. Product distribution and kinetic data were used to postulate the reaction pathway. A reaction pathway over the promoted iron catalyst initiated by the formation of the "enol" intermediate, Eq. (5), from chemisorbed hydrogen and carbon monoxide was proposed by Pichler and Kruger (1973).

$$H\text{--}M + O=C=M \longrightarrow HO-CH=M + M \qquad (5)$$
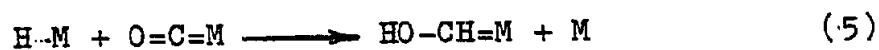
It was well known that at reaction temperature hydrogen has a high tendency to chemisorb dissociatively over a metal

catalyst. Infrared studies (Eischens and Pliskin, 1958) have shown that the only observed form of chemisorbed carbon monoxide over a iron catalyst was the linear structure. The "enol" intermediate can be viewed as the monomer for the oligomerization. Hydrocarbons and oxygenates were produced by hydrogenation and dehydration of the "enol" intermediates, Eq. (6 to 10).

Chain Initialization

$$2\ HO-CH=M\ \xrightarrow[+2\ H-M]{-H_2O}\ CH_3-COH=M \qquad (6)$$

Chain Growth

$$R\ COH=M\ +\ HO-CH=M\ \xrightarrow[+2\ H-M]{-H_2O}\ R-CH_2-COH=M \qquad (7)$$

Paraffin Formation

$$R-CH_2-CHOH=M \xrightarrow[+2\ H-M]{H_2O} R-CH_2-CH_2-M \xrightarrow{+H-M}$$

$$R-CH_2-CH_3 \qquad (8)$$

Olefin Formation

$$R-CH_2-CH_2-M \xrightarrow{-H-M} R-CH=CH_2 \qquad (9)$$
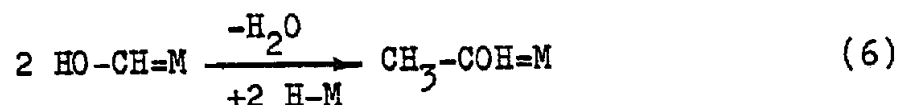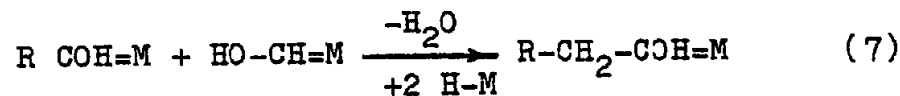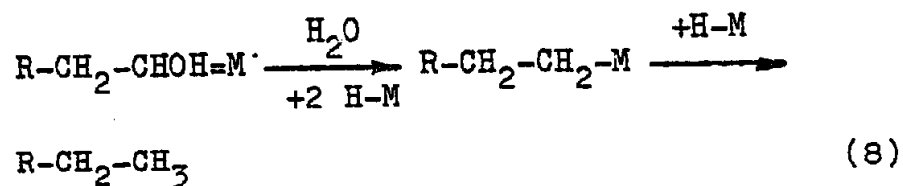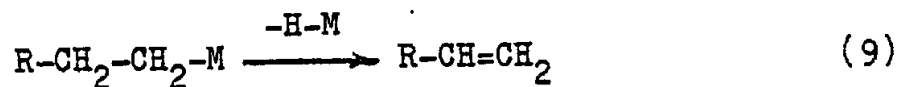
Methyl Branching and Oxygenate Formation

$$R-HCOH-M + HO-CH=M \xrightarrow[+ 2H-M]{-H_2O} R-C(CH_3)OH-M + H-COH=M$$

$$\xrightarrow[+H-M]{-H2O} R-CH(CH_3)-COH=M$$

$$\xrightarrow{+2\ H-M} R-CH(CH_3)-CH_2-OH$$

$$\xrightarrow{-M} R-CH(CH_3)-CHO \qquad (10)$$
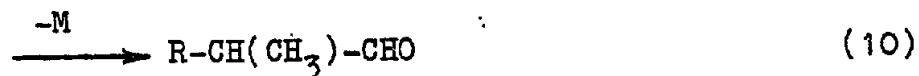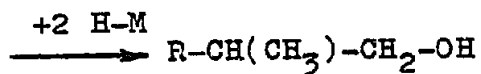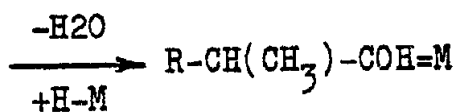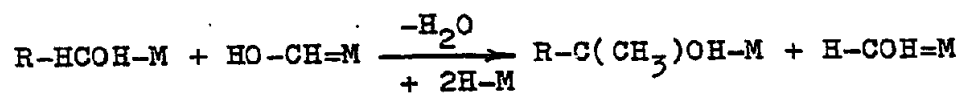
Generally, the hydrocarbons and oxygenates produced from Fischer-Tropsch catalyst were ranged from C_1 to C_{11}^+. Numerous review articles and books have been published which describe various aspects of the Fischer-Tropsch process. In summary, the main disadvantage of the Fischer-Tropsch Synthesis was the non-selective nature of the product.

Methanol Synthesis

Early research on hydrocarbon synthesis from synthesis gas led to the development of methanol synthesis in 1922 (Baird, et al.). Today, the U.S. annual production rate of methanol from synthesis gas is over one billion gallons (Editors, Ch. & Eng. News, 1977) Methanol is an important industrial solvent, and it is used as the starting material for many commercial products, notably formaldehyde. Recent interest in alternative hydrocarbon synthesis has placed an even greater importance upon synthesis gas derived methanol, since methanol could be converted to hydrocarbons selectively.

The overall methanol synthesis reaction is:

$$CO + 2 H_2 \longrightarrow CH_3OH \tag{11}$$
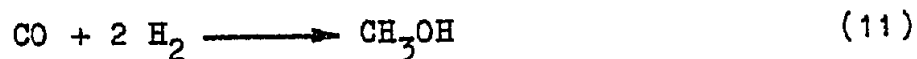
Thermodynamics of the methanol synthesis reaction favor low reaction temperature and high pressure, but a higher temperature was required to have a sufficient activity. Thus, an active low temperature catalyst was sought.

Industrial methanol catalysts are classified into high pressure and low pressure type. The high pressure catalysts will be the supported zinc oxide , and the low pressure catalysts will be the mixed copper-zinc oxide. The operating conditions for the mixed copper-zinc oxide catalysts are much milder than the high pressure catalysts,

but the low pressure catalysts are very sensitive to sulfur poisoning, Eq. (12), and thermal shocks, according to Natta (1955).

$$Cu + H_2S \longrightarrow CuS + H_2 \qquad (12)$$
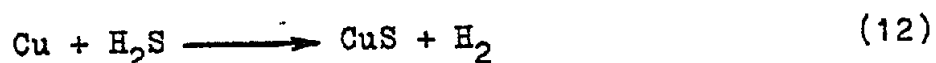
Although the methanol synthesis reaction appears to be rather simple, the reaction mechanism is very much in dispute. It is known that if the reactant stream contains no carbon dioxide or water, there will be much less methanol production. Furthermore, most methanol synthesis catalysts, low or high pressure type, will also catalyze the water gas shift reaction. Consequently, it was suggested by Rozorskii, et al. (1975) that the water gas shift generated carbon dioxide was the real precursor for methanol synthesis, according to Eq. (13)

$$CO + H_2O \longrightarrow CO_2 + H_2 \xrightarrow{+2\ H_2} CH_3OH + H_2O \qquad (13)$$
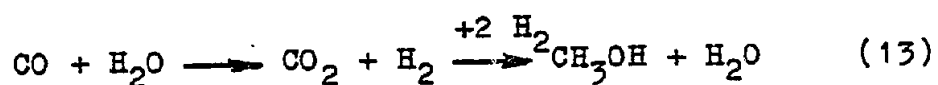
Recent articles (Herman, et al., 1979, and Kung, 1980) have disregarded this mechanism based on two main observations. First, the hydrogenation of carbon dioxide is thermodynamically less favorable than hydrogenation of carbon monoxide. Second, the water gas shift reaction rate is not substantially higher than the rate of methanol

production on most methanol synthesis catalysts. Herman, et al. (1979) and Kung, (1980) suggested that carbon dioxide and water were used to protect the active sites of the catalyst from reduction by synthesis gas during the reaction. Presently, there are several proposed mechanisms for methanol synthesis (Nagarjinan, et al., 1963, Herman, et al., 1979, and Kung, 1980). Nagarjunan, et al. (1963) proposed Mechanism I, Figure 1, in which the first step of the reaction was the formation of a surface formate from surface hydroxyl and carbon monoxide

Mechanism I

$$CO \xrightarrow{+M} M-CO \xrightarrow{+ M-O-H} M-O-CH=O$$

$$\xrightarrow{+2 \ M-H} M-O-CH_2-OH \xrightarrow{- H_2O} \xrightarrow{+2 \ M-H}$$

$$M-O-CH_3 \xrightarrow{+M-H} M + CH_3OH$$
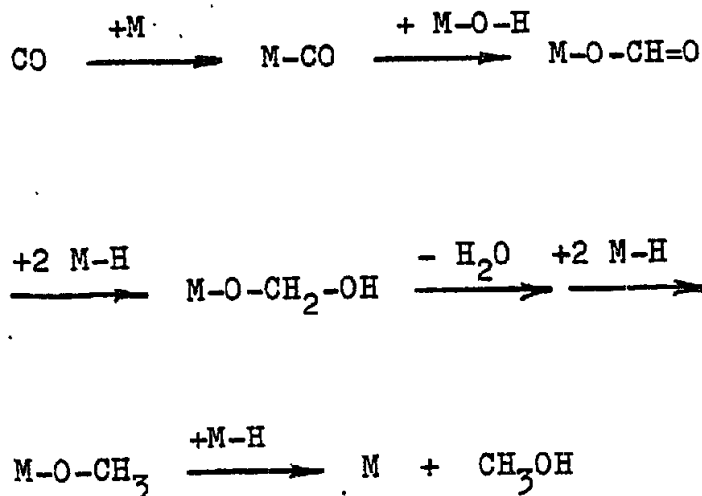
Figure 1. Methanol Synthesis via Surface Oxygen Exchange

That was followed by hydrogenation and dehydration to form a surface methoxide which was hydrogenated to methanol. But, there was insufficient evidence to suport the first step of the reaction, carbon monoxide insertion into the surface hydroxyl, and the multistep of hydrogenation and dehydration of a surface intermedate.

Kung (1980) proposed that the interaction between the surface oxygen vacancy site of zinc oxide catalyst and chemisorbed carbon monoxide played an essential role in the carbon monoxide activation, Mechanism II. The oxygen vacancy sites of zinc oxide were created during the calcination process, according to Eq. (14).

$$2Zn^{2+} + 2O^{2-} \longrightarrow O_2 + 2Zn^O \quad (14)$$
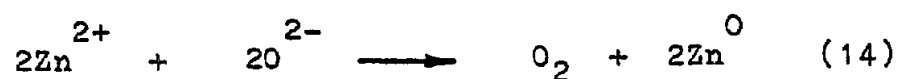
It was well known that zinc oxide will undergo Eq. (II-14) to become a n-type semiconductor. In Mechanism II the active catalytic site was proposed to be a cluster of zinc ions and atoms surrounding a surface oxygen vacancy site which was denoted as V in Figure 2. The reaction pathway began by the chemisorption of hydrogen and carbon monoxide. The surface oxygen vacancy site interacted strongly with the carbon monoxide's oxygen to stabilize and substantially activate the chemisorbed carbon monoxide species. Then, the surface carbon monoxide was sucessively hydrogenated to form the surface formyl and methoxide species, respectively. The

Mechanism II

O
•O
Zn
V
Zn-----Zn

−CH₃OH / 5 ... +2H₂

1

CH₃
O
O
Zn—O
V   H
Zn-----Zn

H   H
O
Zn   O
H / V \ H
Zn-----Zn

4 ... 2 | +CO

H
O=C
H   H
O   O
Zn
V   H
Zn---- Zn

3

O≡C
H   H
O   O
Zn
H / V \ H
Zn-----Zn
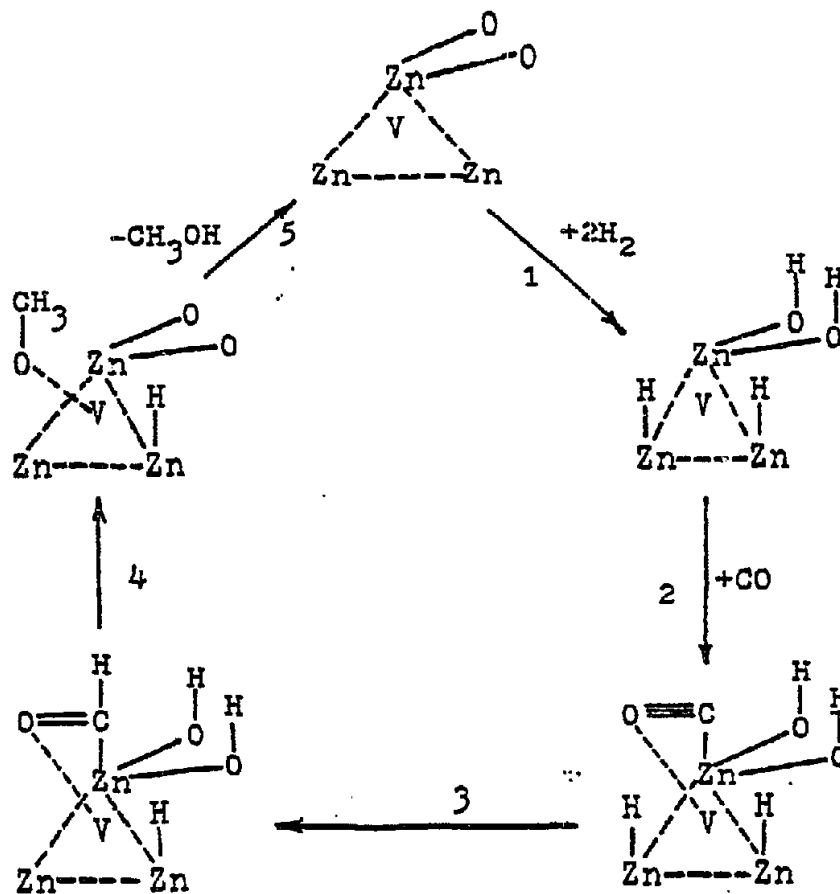
V= Surface Oxygen Vacancy Site

Figure 2.   Methanol Synthesis via Surface Oxygen Vacancy

surface methoxide was subsequently hydrogenated to methanol.
In this proposed mechanism all surface intermediates were
stablized by the surface oxygen vacancy site. This proposed
mechanism was supported well by experimental data, and it
served as a good working model for the methanol synthesis
over zinc oxide, a high pressure catalyst. But, the Kung
model did not address the reaction pathway for the mixed
copper-zinc oxide catalysts.

The mixed copper-zinc oxide catalyst with its
limitations to sulfur poisoning and thermal shocks is still
the most wildly used commercial catalyst because of its high
activity at low pressure. Herman, et al. (1979) postulated
that the active catalytic phase of mixed copper-zinc oxide
was the oxide solution of copper-zinc, Cu(I)/ZnO, and it was
not the individual metal oxides. Herman, et al. (1979)
proposed a reaction mechanism for methanol production over
mixed copper-zinc catalysts, Figure 3. The mechanism can be
characterized overall as the sucessive hydrogenation of
adsorbed carbon monoxide with no exchange of oxygen. The
main feature of this mechanism was the mutual enhancement
effect of the oxide solution in synthesis gas adsorption.
The selective adsorption of synthesis gas onto the oxide
solution was aided by the selective affinity of carbon
monoxide and hydrogen to copper and zinc, respectively
(Herman, et al., 1979).

Each proposed mechanism had its own unsatisfactory
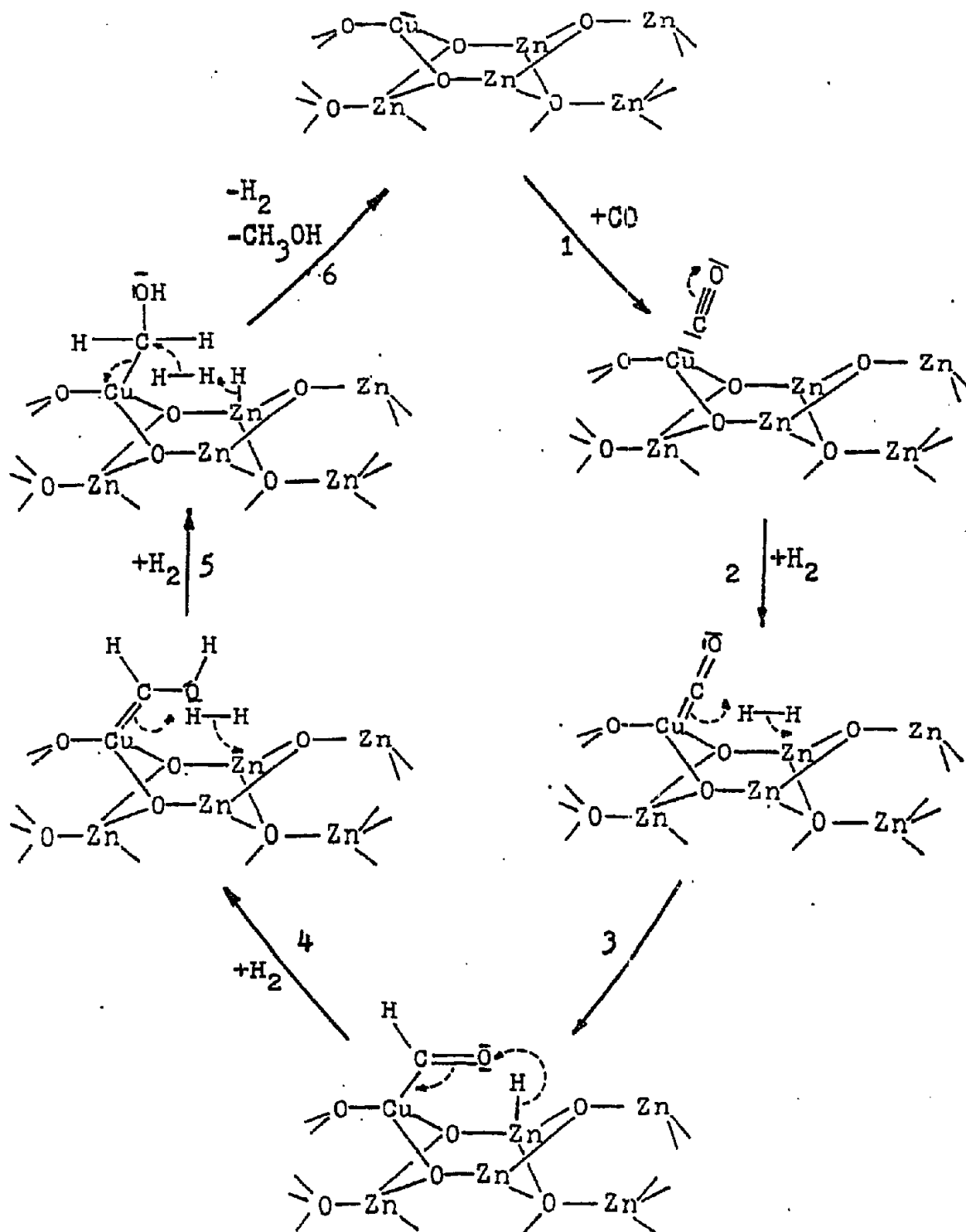
Figure 3. Methanol Synthesis via Surface Oxide Solution

aspects such as the role played by the surface oxide oxygen, the possibility of oxygen exchange, the formation of methane, and the accountability for the water gas shift reaction.

Methanol Conversion to Hydrocarbons

Catalytic conversion of methanol to hydrocarbons was the only new technology to obtain hydrocarbons indirectly from synthesis gas since the the closing of all Fischer-Tropsch plants everywhere except in South Africa more than forty years ago. In 1962 Mattox reported the production of hydrocarbons during methanol dehydration to dimethylether over NaX zeolite. The Mattox report stimulated great interests thus resulting in the birth of current methanol technologies for producing hydrocarbons from methanol.

Currently, there are two major related approaches to convert methanol to hydrocarbons selectively, the Mobil MTG process (methanol to gasoline) and the methanol to light olefins process. The main difference between the two processes was the catalysts involved. The reaction pathways for the two processes were the same, Eq. (15).

$$CH_3OH \xrightarrow[\text{Step 1}]{-H_2O} (CH_3)_2O \xrightarrow[\text{Step 2}]{-H_2O} (CH_2)_n \qquad (15)$$
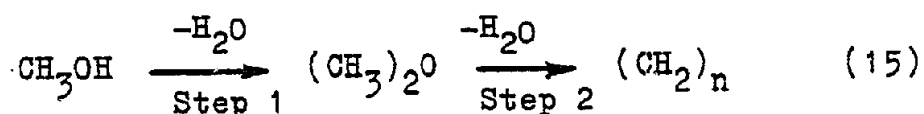
The different hydrocarbons obtained from the two processes were the consequence of the extent of oligomerization in Step 2 which was affected by the shape selective catalyst. The catalysts involved in the two processes were zeolite of appropriate geometry and pore size. The catalyst used for the Mobil MTG process (Chang, et al. 1979) was a medium pore size (7 Å) zeolite, ZSM5, with a high Si/Al ratio of 15, and for the methanol to light olefin process was a small pore size (4 Å) zeolite, chabazite, with a Si/Al ratio of 1.6.

The effects on the product distribution by the different zeolites were clearly shown in TABLE 1.

TABLE 1. Comparison of Product Distributions

Product (wt.%)	Catalyst		
	F-T [1]	ZSM-5 [2]	Chabazite [3]
Light gases (C_1-C_2)	11	2	57
L.P.G. (C_2-C_3)	11	22	43
% Olefin (C_2-C_3)	–	–	60
Gasoline (C_5^+)	25	76	–
Fuel Oil (C_{11}^+)	51	–	–
Oxygenates	2	–	–

[1] SASOL Process (Fruhning and Cornils, 1974)
[2] Mobil Process (Chang, et al. 1978)
[3] Light Olefin Process (Singh, 1980)

The products from chabazite were predominantly light olefins and paraffins (C_2 to C_4), where as the products from ZSM-5 catalyst were gasoline range hydrocarbons (C_5 to C_{11}) of high aromatic content. TABLE 1 also clearly showed the high selectivity of the zeolite based processes over the poor selectivity of the Fischer-Tropsch process.

Zeolite as Methanol to Hydrocarbon Catalyst

Since much of the recent studies on methanol conversion to hydrocarbons were conducted using zeolite as catalyst, it was necessary to examine the catalytic properties of zeolite. Catalytic properties of zeolite for methanol to hydrocarbon can be generally separated into two categories, namely the molecular sieving effect and the surface acidity effect.

Zeolites were a class of hydrated aluminosilicates which upon heating will develop into a crystal of uniform pore size and channel system. The molecular sieving effect of zeolite was the consequence of the ability of molecules to diffuse in and out of the zeolite matrix. This effect was demonstrated by the ability of zeolite to separate normal from isoparaffin.

The active catalytic sites for methanol conversion to hydrocarbons have been generally accepted to be the strong acidic sites in the zeolite matrix. The acidic sites can be

differentiated into two kind, the Bronsted and Lewis acid. Transformation between the two kinds of acid was depicted in Figure 4.
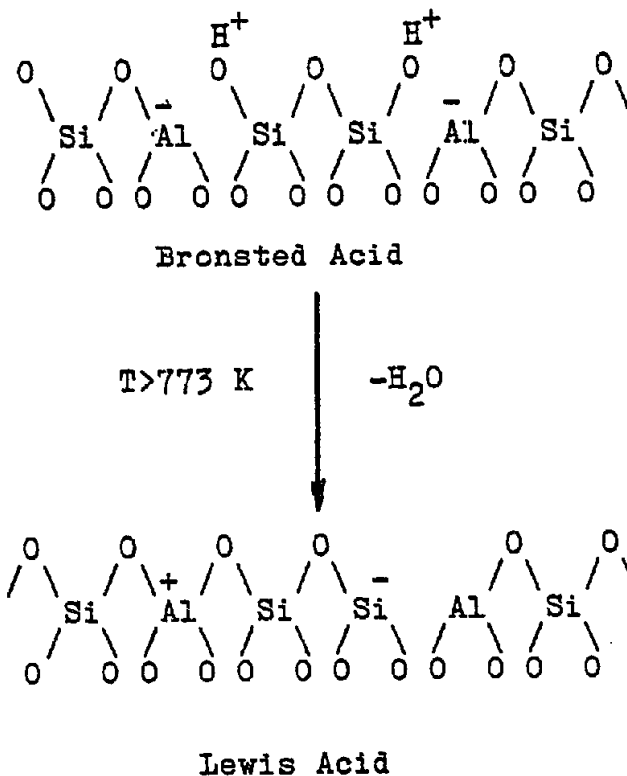
Figure 4. Transformation between Lewis and Bronsted Acid

The acidity in most zeolites was introduced by two methods, namely ammonium ion and polyvalent ion exchange, Figure 5 and Figure 6. The polyvalent cation exchanged zeolite will have a higher collapse temperature for the zeolite matrix than the ammonium exchanged zeolite at the same degree of exchange. However, the polyvalent cation exchanged zeolite

will have fewer acid sites than the ammonium exchanged zeolite. The most often used cations in polyvalent cation exchanged procedure were a mixture of rare earth chlorides.
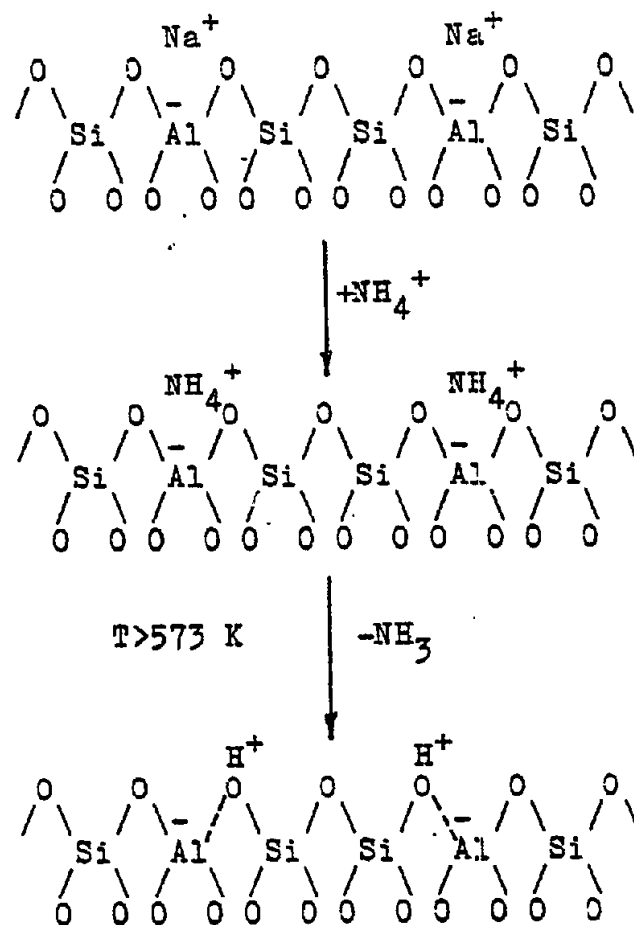
Figure 5. Acid Introduction by Ammonium Exchange
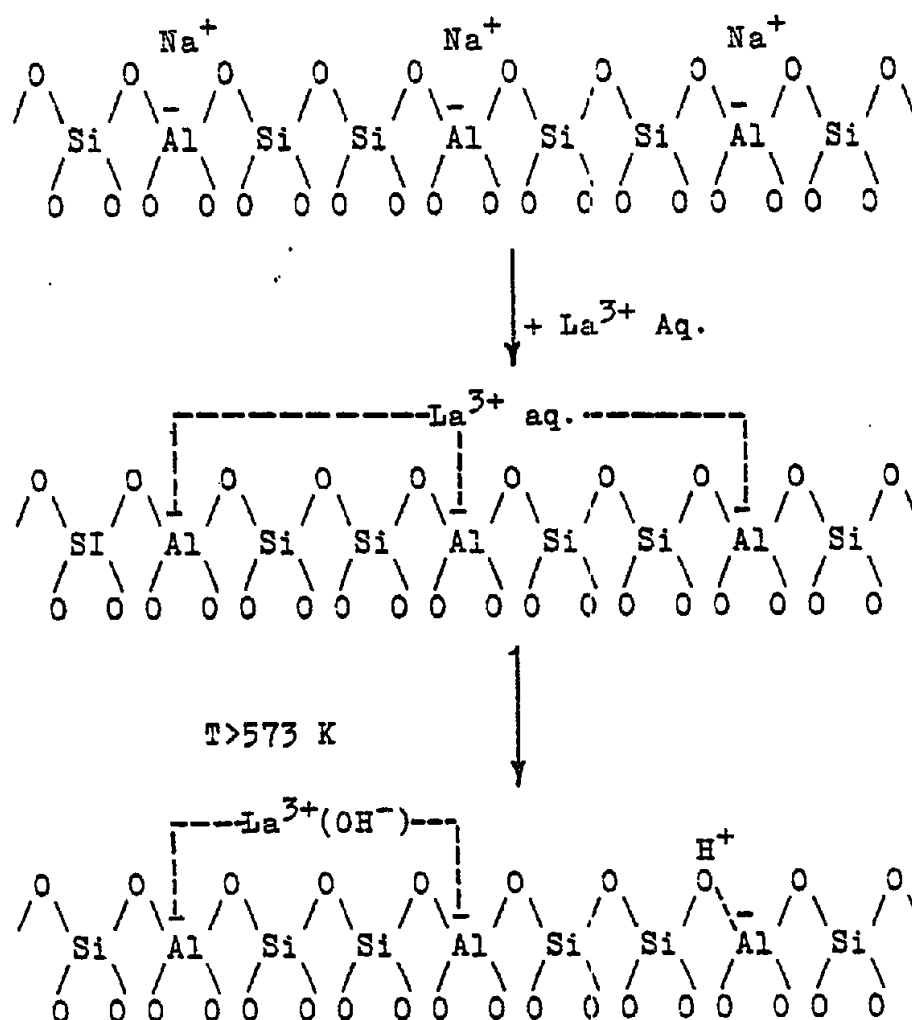
Figure 6. Acid Introduction by Rare Earth Cation Exchange

CHAPTER III

CATALYST PREPARATION

Since the major objective of this work was to incorporate the methanol synthesis and methanol decomposition function on the same catalyst particle, it is important to detail the technique used for catalyst preparation. Three different techniques were used in this study. A list of all raw materials used in the procedure was provided in APPENDIX B. A detailed description of all catalysts used was given in TABLE 2.

Ammonium and Rare Earth Ion Exchange Procedure

Zeolon-500, a mixture of erionite and chabazite, and pure erionite were ion exchanged for the generation of surface acidity. The procedure used in the ion exchange was obtained from Singh (1980).

1. Zeolite powder was washed with deionized water (20 wt.%) three times.

2. A 0.3 molar rare earth choride solution and a 0.5 molar ammonium choride solution were prepared.

3. The washed zeolite powder was then transfered into a three neck flask, and 2.5 cc of rare earth and ammonium choride solution per gram of zeolite were added.

4. The solution was refluxed for 96 hr.

5. After reflux the ion exchanged zeolite was filtered and washed with deionized water three times.

6. The zeolite was then dried overnight in a 373 K oven.

TABLE 2 Catalyst Description

Designation	Technique*	Methanol Synthesis Catalyst Precursor	Zeolite Component	Calcination Temperature
Cat. 1	A	Zinc Chromite** (2.8 gm.)	Zeolon*** (2.81 gm.)	None
Cat. 2	A	Zinc Chromite** (27.01 gm.)	Erionite**** (25.11 gm.)	723 K
Cat. 3	B	$Zn(NO_3)_2 \cdot 6H_2O$ (2.51 gm.)	Erionite**** (10.91 gm.)	876 K
Cat. 4	B	$Zn(NO_3)_2 \cdot 6H_2O$ (57.2 gm.)	Erionite**** (80.2 gm.)	811 K
Cat. 5	B2	$Cu(NO_3)_2 \cdot 3H_2O$ (2.18 gm.) $Zn(NO_3)_2 \cdot 6H_2O$ (4.07 gm.)	Erionite**** (21.7 gm.)	755 K
Cat. 6	C	$Cu(NO_3)_2 \cdot 3H_2O$ (111.0 gm.) $Zn(NO_3)_2 \cdot 6H_2O$ (310.2 gm.)	Erionite**** (122.1 gm.)	673 K

* A = Physically Mixed
  B = Impregnation
  B2 = Co-impregnation
  C = Co-precipitation

** Harshaw, Zn-0132, batch 69
*** Ammonium, rare earth exchanged erionite and chabazite mixture
**** Ammonium and Rare Earth Exchanged

Physically Mixed Catalyst Preparation Procedure

The simplest method for testing the cooperative action of methanol synthesis catalyst and methanol decomposition catalyst was to place an intimate mixture of the two catalyst components into the reactor. Cat.1 and Cat.2 were prepared using this physically mixed method. The detailed procedure was the following:

1. Each catalyst component was ground separately to the desired particle size.
   (Cat.1: Zinc Chromite = 145-155 micron,
            Zeolon-500   = 75-85   micron.
     Cat.2: Zinc Chromite = 75-85 micron,
            Erionite   = 44-53 micron.)

2. Each catalyst component was weighed then the catalyst components were throughly mixed in a vial.

3. Solvent such as water or methanol was added to the catalyst mixture slowly until a thick and consistent paste was obtained.

4. The particle paste was then placed into a 20 cc syringe with a 1/8 inch opening for extrusion.

5. The extrudates were then placed in an oven, Precision-Thelco Oven, for 2 hr. at 373 K.

6. The dried extrudates were transferred into a 2 inch I.D. stainless tube for calcination.

7. The 2 inch I.D. stainless steel tube was placed inside of a Hoskins Electric Furance, and air supplied from a cylinder was fed into the tube.

8. The air flow rate was maintained at 20cc/min. for 2 hr.

Impregnation Procedure

As in most non-trivial polyfunctional catalysts, the intimacy of individual components was an important factor in the total performance of the polyfunctional catalyst. Interparticle heat and mass transfer resistance can be substantialy reduced by an increase in the degree of intimacy between each catalyst component. Thus, the impregnation of methanol synthesis component into the zeolite matrix was studied. Cat.3, Cat.4, and Cat.5 were prepared using the impregnation method. The impregnation and coimpregnation procedures were the following:

1. A 1.0 molar solution of $Zn(NO_3)_2$ and of $Cu(NO_3)_2$ were prepared.

2. The 1.0 molar $Zn(NO_3)_2$ and/or $Cu(NO_3)_2$ solution were slowly added to the predetermined amount of zeolite.

3. The zeolite paste was throughly mixed.

4. The zeolite paste was transfered to a 20cc syringe for extrusion.

5. The extrudates were dried in a 373 K oven for 2 hr.

6. The dried extrudates were calcined using the procedure given in the physically mixed technique.

Coprecipitation Procedure

The impregnation technique can only be used for catalyst preparation with low loading level. For high loading level catalyst, the most used method of preparation was the precipitation technique. Cat.6 was prepared using the following procedure.

1. A 1.0 molar solution of $Cu(NO_3)_2$ and $Zn(NO_3)_2$ was prepared.

2. The nitrate solution was heated to 358 to 363 K in a three neck flask.

3. A predetermined amount of zeolite was added into the nitrate solution.

4. Under stirring a sodium carbonate solution was added dropwise until the pH=7.

5. After precipitation the precipitate was filtrated and washed with deionized water three times.

6. Deionized water was added to the precipitate until a thick and consistent paste was obtained for extrusion.

7. The extrudates were dried in a 373 K oven overnight

8. The dried extrudates were calcined using the procedure given in the physically mixed method.

CHAPTER IV

EXPERIMENTAL APPARATUS

The experimental appartus used in this study was a high pressure continuous flow system. The system was designed to accommodate both gas and liquid feed simultaneously. The apparatus was composed of three main sections, namely the feed system, the reactor, and the analytical section. A schematic drawing of the apparatus was provided, Figure 7.

Feed System

The feed system consisted of two parts, gas and liquid feed. Liquid drawn from a buret (W) was fed into the liquid pump, and the liquid feed rate was controlled by the pump, Milroyal-D Controlled Volume Pump (T). A pressure gauge and a check valve were placed in the exit of the liquid pump to determine the head pressure of the pump and to prevent gas back-up, respectively. High pressure liquid from the liquid pump was then mixed and vaporized with reactant gases in the preheater (K) before entering the reactor (L).

The gas feed section consisted of individual gas cylinders (A-E), an air operated compressor (F), a mixing tank (G), gas purifiers (H-I), and a mass flow meter and controller (J). The gas feed system was designed to prepare gas mixtures of various compositions and pressures. Individual gas was connected to the American Instrument air-operated compressor for mixing and compression.
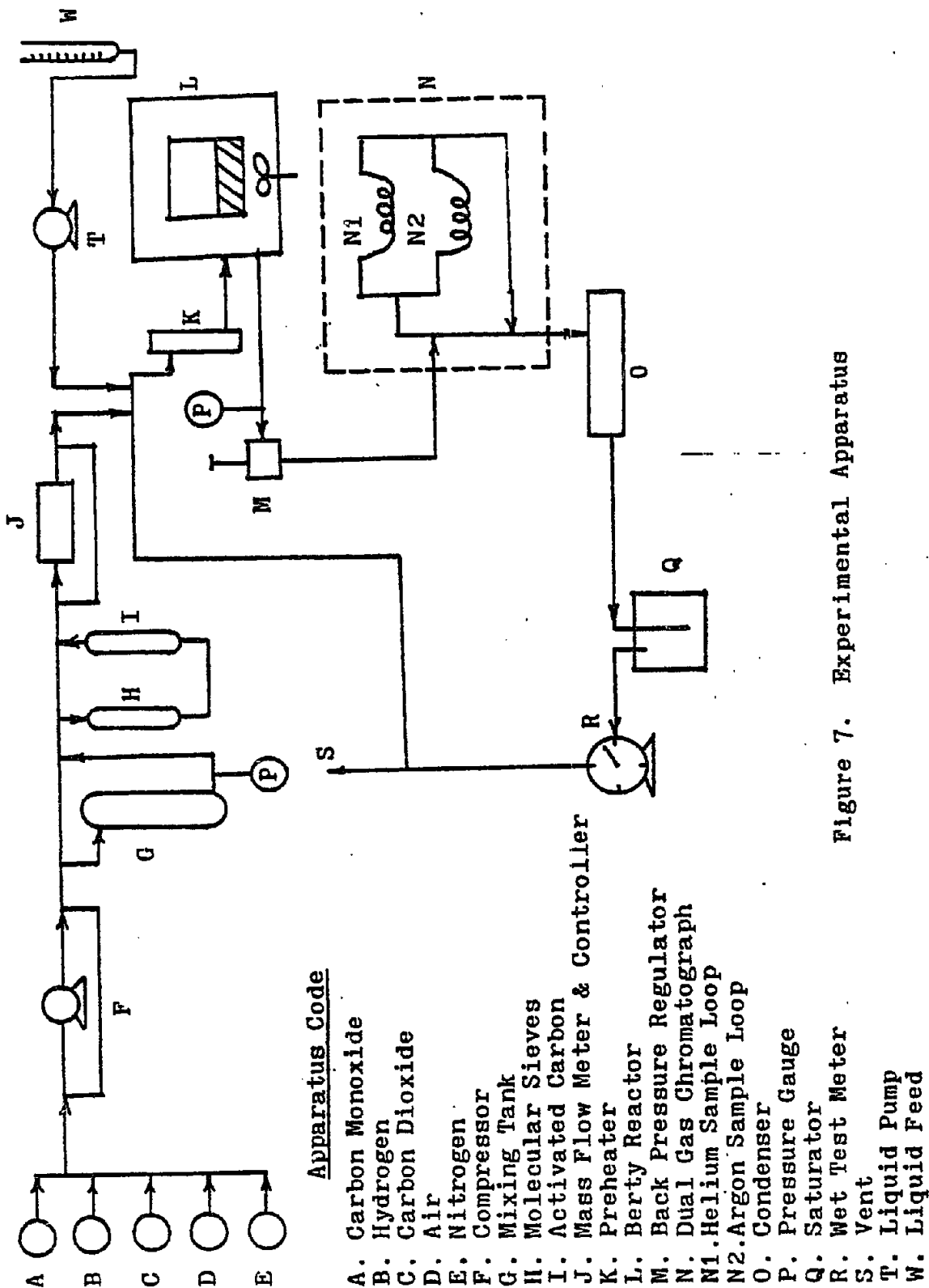
Figure 7.   Experimental Apparatus

Apparatus Code

A. Carbon Monoxide
B. Hydrogen
C. Carbon Dioxide
D. Air
E. Nitrogen
F. Compressor
G. Mixing Tank
H. Molecular Sieves
I. Activated Carbon
J. Mass Flow Meter & Controller
K. Preheater
L. Berty Reactor
M. Back Pressure Regulator
N. Dual Gas Chromatograph
N1.Helium Sample Loop
N2.Argon Sample Loop
O. Condenser
P. Pressure Gauge
Q. Saturator
R. Wet Test Meter
S. Vent
T. Liquid Pump
W. Liquid Feed

A sample of the gas mixture in the mixing tank was obtained at the sample valve located at the tank exit for composition analysis by gas chromatograph. A pressure gauge also was placed at the mixing tank exit to determine the amount of gas in the tank. The gases were then passed through a set of gas purifiers which consist of activated carbon (I) and molecular sieve (H). A Brooks Mass Flow Meter and Controller was employed to measure and control the gas flow rate into the preheater. Calibrations of different gases for the mass flow meter were accomplished with the aid of a water saturator (Q) and a wet test meter (R). Finally, a condenser (O) was used to remove excess liquid from the reaction effluent at room temperature before venting.

Reactor System

The reactor system consisted of a Berty gradientless reactor (Figure 8), a furnace, a temperature controller, and a back pressure regulator (M). Reactants were fed into the reactor from the preheater. The heating of the reactor was accomplished by using a three zone Autoclave furance, and the temperature of the reactor was controlled by a Thermolyne Solid State Temperature Controller. The pressure of the reactor was maintained by a Veriflo, spring loaded, back pressure regulator. All lines entering and leaving the reactor were heated by heating tape and insulated with asbestos cloth tape to prevent condensation.
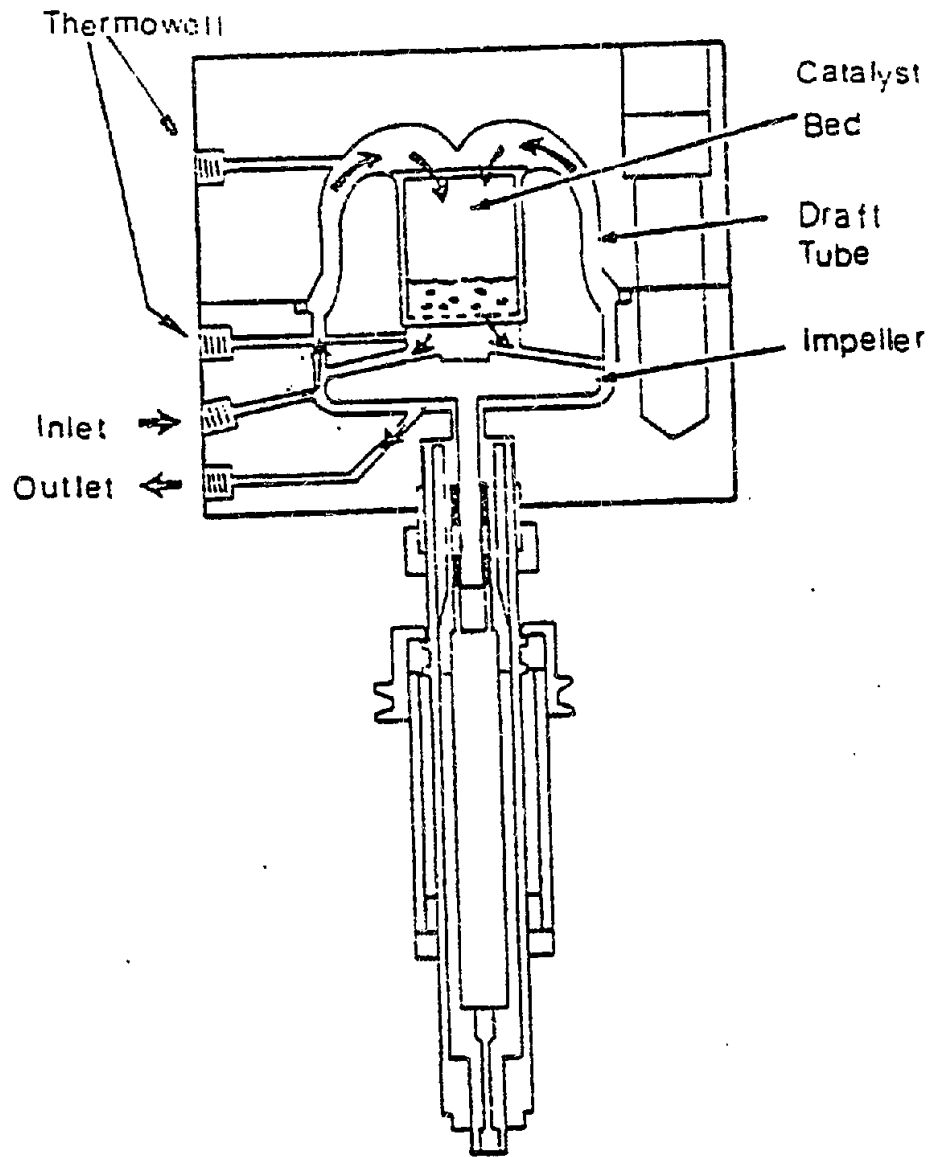
Figure 8. Berty Reactor

The Berty gradientless reactor employed in this study was classified as a perfectly mixed flow reactor since the gas and solid composition, pressure, and temperature were essentially uniform through out the reactor. The design and the details of the reactor was reported by Berty (1974). The perfectly mixed flow reactor characteristics were obtained by the high internal recirculating of reaction fluid. Advantages of using a Berty reactor were:

 i. Differential kinetic data.

 ii. Simulation of local conditions in an integral reactor

 iii. Improved external heat and mass transfer.

 iv. Uniform poisoning of the catalyst resulting from uniform environment surrounding the catalyst particle.

 v. Isolation of possible reaction intermediate products

Analytic System

The reaction effluent was analyzed using a dual gas chromatograph (N). Quantitative analysis of hydrocarbons and oxygenates were conducted using a Gow Mac thermal conductivity gas chromatograph where helium was used as the carrier gas. The column used to separate the hydrocarbons and oxygenates was a 10 ft. long x 1/8 inch O.D. stainless steel column packed with 100-120 mesh of Porapak Q. Peak area integrations were made by a Varian CDS-111 digital integrator.

p

Permanent gas analysis was conducted using a Barber Colman thermal conductivity gas chromatograph with argon carrier gas. The separation column used for this analysis was a 5 ft. long x 1/4 inch O.D. stainless steel column packed with 60-80 mesh of 5 A molecular sieves. Integration was made by a CRS-104 digital integrator.

The sampling apparatus for gas chromatograph analysis consisted of two 6-port Carle Sample Valves. The configuration of the sampling system was given in Figure 9.
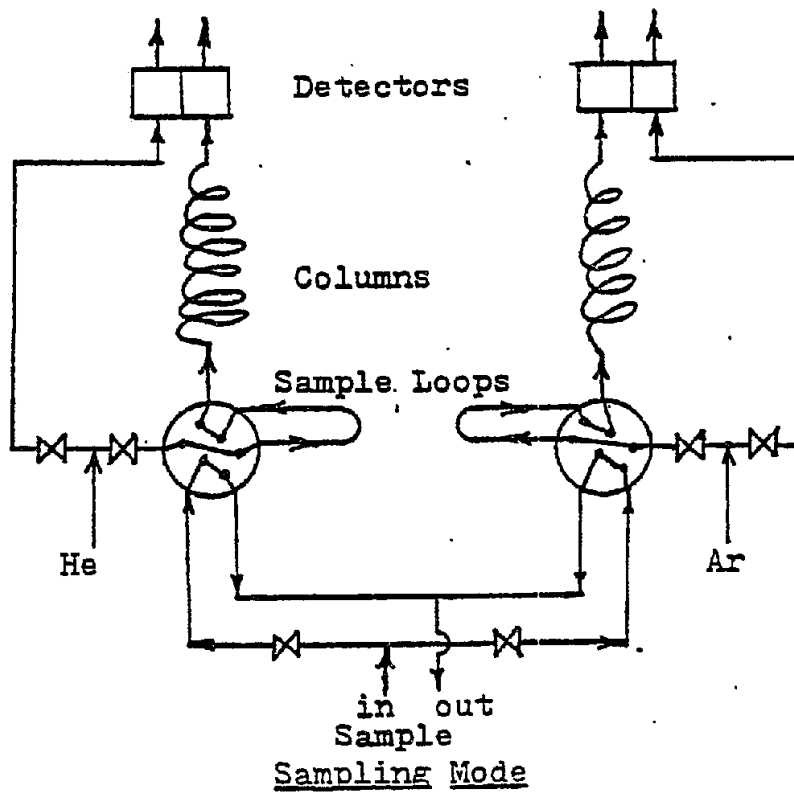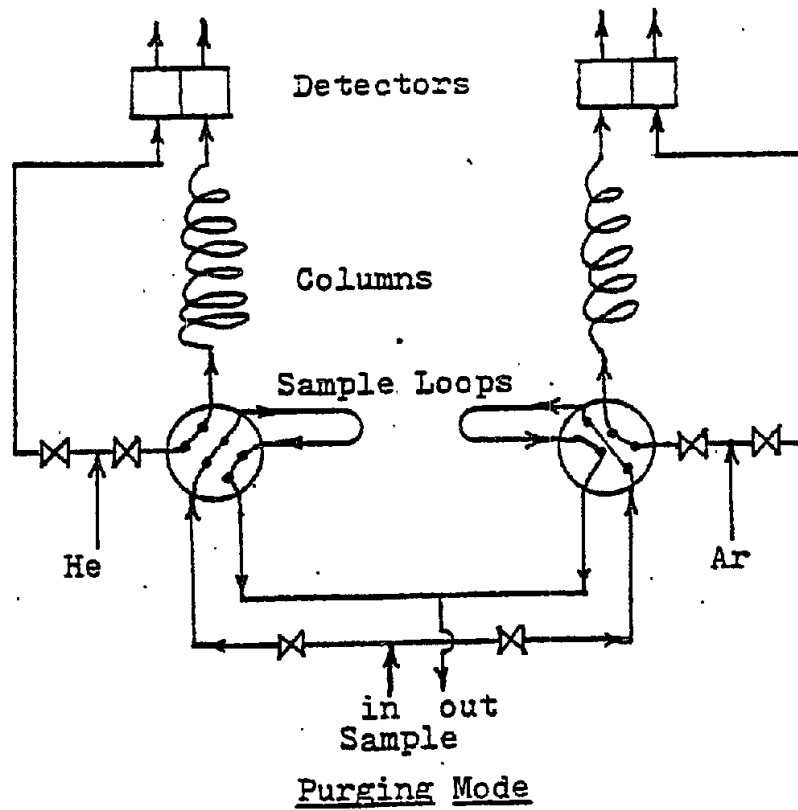
Figure 9. Sampling Apparatus

CHAPTER V

EXPERIMENTAL PROCEDURE

Catalytic testing procedures consisted of start up, steady state operation, and product analysis. Furthermore, a detailed history for each catalyst was recorded for the purpose of explaining any unexpected anomaly.

Start Up Procedure

1. A predetermined amount of catalyst was placed into reactor.

2. The reactor was closed according to the procedures recommended by the reactor manufacturer, Autoclave.

3. The reactor was then purged with nitrogen. The pressure of the reactor was increased to above the reaction pressure, and the reactor was isolated by closing the inlet and outlet for the purpose of leak test which was indicated by the pressure drop. Reactor enclosure was slightly tightened until the pressure drop was below 2 psi/hr.

4. Gas chromatographs, heating tapes, and reactor furnace were activated.

5. When reaction temperature was attained the mass flow meter and controller was then opened and set to slowly introduce reactant gases into the reactor.

6. The back pressure regulator was adjusted until reaction pressure was reached, then the reactor

impeller was activated.

Steady State Operation

When reactor temperature and pressure have stablized, preliminary analysis of reaction product was made to test for steady state operation. After steady state operation criteria were satisfied, the impeller speed was increased until there was no change in methanol conversion. The increase in recirculating rate was made to insure the reaction was not in the external mass transfer controlled region. When the criterion of internal processes controlling was satisfied, complete product analysis was then initialized.

Product Analysis Procedure

Analysis of hydrocarbons and oxygenates was conducted using a Gow Mac gas chromatograph using helium as the carrier gas. In this analysis the column temperature was programmed to shorten the analysis time and to better separate the products. The column temperature was at 296 K during the elution of CO, CH_4, and CO_2, then the column temperature was increased to 473 K for the elution of remaining products. Permanent gas analysis under the Barber Colman gas chromatograph was carried out isothermally. The operating parameters for the two gas chromatographs were:

Gow Mac		Barber Colman	
He Flow Rate	=30cc/min.	Argon Flow Rate	=35cc/min.
Detector Temp.	=473 K	Detector Temp.	=473 K
Detector Current	=200mA	Detector Current	=75mA
		Column Temp.	=373 K

Regeneration Procedure

Regeneration of catalyst was carried out using cylinder air. The procedure that was used in regeneration was the same procedure used in catalyst testing except the reaction pressure was kept at 50 psig and reaction time was much longer.

CHAPTER VI

DISCUSSION OF CATALYTIC TESTING RESULTS

Catalytic tests for hydrocarbon production from synthesis gas were performed on each prepared catalyst using the procedure given in CHAPTER V. A tabulation of all catalytic testing data were given in APPENDIX A. Catalytic testing results showed that methanol was indeed produced by all of the tested catalysts. Presence of methanol in the reaction effluent indicated that the methanol synthesis component of the bifunctional catalyst was active. The concentration of methanol was low compared to the other products. The low concentration of methanol was consequence of the pressure limitation on the methanol synthesis reaction and the draining effect of methanol decomposition to hydrocarbons. The conversion of methanol was far from equilibrium conversion limit. Dimethylether was also observed in the product, and its formation was attributed to the dehydration of methanol. The conversion of methanol to dimethylether was not at equilibrium limit.

In all runs the hydrocarbons were observed in the product, and the hydrocarbons were between C_1 and C_4. Production of hydrocarbons indicated that the zeolite component of the bifunctional catalyst was active in conversion of methanol to hydrocarbons. The narrow product distribution of the hydrocarbon fraction was indicative of

the shape selectivity of the zeolite used in the catalyst. The water gas shift reaction was observed to be in dynamic equilibrium in all runs. Experimental runs with carbon dioxide in the feed (Run # 4.3 to 4.5) showed the retarding effect of carbon dioxide on hydrocarbon production.

A representative comparsion of activity and selectivity for the tested catalyst was shown in Figure 10. Of all the catalysts studied Cat. 3, erionite impregnated with ZnO, was shown to have the highest activity and selectivity for hydrocarbons compared to other catalysts at similar conditions. The main feature in the hydrocarbon fraction of the product as shown in Figure 10 was the large amount of paraffinic hydrocarbons compared to the olefinic hydrocarbons. Two possible explanation for the small olefinic content in the hydrocarbon fraction was examined. First, the formation of olefins and paraffins was independent of each other. Second, paraffins were produced from the hydrogenation of olefins. Much of the recent studies on hydrocarbon formation by methanol decomposition over acidic zeolite have suggested that olefins were the primary products rather than paraffins (Jacobs, 1977, and Salvador, 1977). Furthermore, no evidence exists to support the independent formation of paraffins and olefins over acidic zeolite from methanol. Therefore, one concludes that the high paraffinic content of the hydrocarbon fraction was due to the hydrogenation of olefin. Moreover,
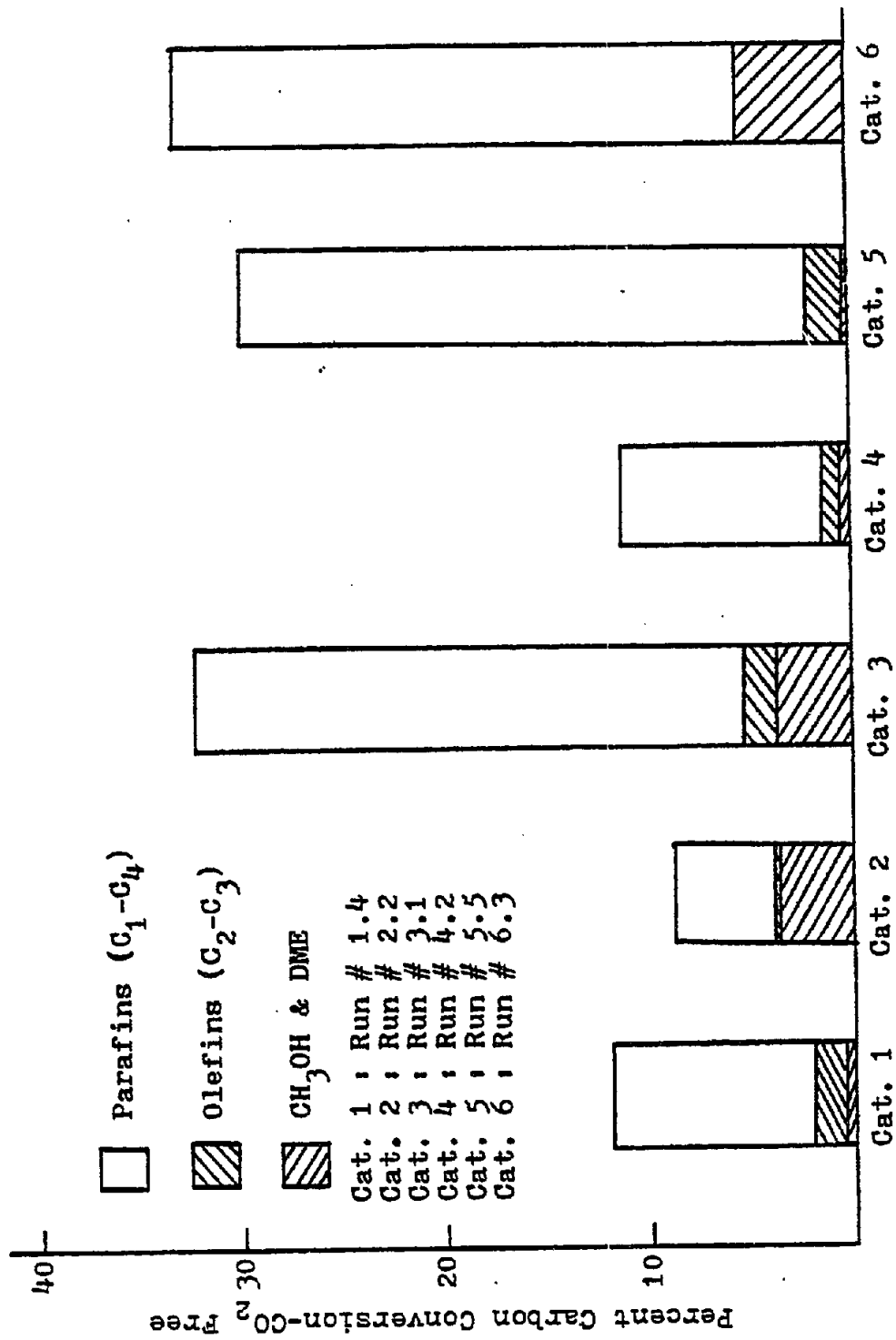
Figure 10.. Catalytic Activity and Selectivity Comparison

experimental Run # 6.9 to 6.15 have clearly demonstrated the olefin hydrogenation characteristic of the bifunctional catalyst. The next question which was addressed was which catalyst component was responsible for the olefin hydrogenation. Results from Run # Z1 to Z5 have shown that the zeolite component of the bifunctional catalyst to have olefin hydrogenation characteristic. However, the extent of hydrogenation by the zeolite component was less than the bifunctional catalyst which indicated that the methanol synthesis component was also active in olefin hydrogenation.

Reaction Mechanism

Of the various proposed mechanisms for hydrocarbon from methanol, the carbenium model fitted well with the catalytic testing results. The carbenium model proposed by Jacobs (1977) and Salvador, et al. (1977) was divided into five consecutive reactions.

1. The formation of dimethylether.
2. The formation of ethene.
3. The formation of higher olefins.
4. The formation of paraffins and cyclic hydrocarbons.
5. The formation of aromatics.

Since the zeolite used in this study was a small pore zeolite then the formation of cyclic, aromatic, and long chain hydrocarbons was highly unfavorable. This was supported by the observation of no cyclic, aromatic, and long chain hydrocarbons in the product. Pictorial description of the formation of dimethylether, ethene, higher olefin, and paraffin were given in Figure 11, 12, 13,

and 14,respectively.

Formation of dimethylether was postulated to be a bimolecular Rideal type surface reaction. Methanol produced by the methanol synthesis catalyst component was chemisorbed onto the surface acid site. The chemisorbed methanol was further reacted with another gas phase methanol, step 2, to form a surface dimethylether species. The surface dimethylether species was then desorbed into the gas phase leaving a adsorbed water molecule which subsequently desorbed. Formation of ethylene was proposed to form by two consecutive Rideal type reactions. First, the surface acidic proton reacted with gas phase dimethylether to form a surface methyl carbonium ion and a gas phase methanol. Second, the surface carbonium ion was reacted further with another dimethylether to form a more stable surface primary carbonium ion which was desorbed as ethylene leaving a surface acidic proton.

The more stable surface primary carbonium ion was proposed to be the starting species for all subsequent reactions such as the formation of paraffins (Figure 13) and higher olefins (Figure 14). Reactivity of this surface primary carbonium ion was the determining factor in the hydrocarbon product selectivity and coking characteristic. Desorption of the carbenium ion led to the formation of ethylene. Reaction of the carbenium ion with gas phase olefins or dimethylether led to the production of higher
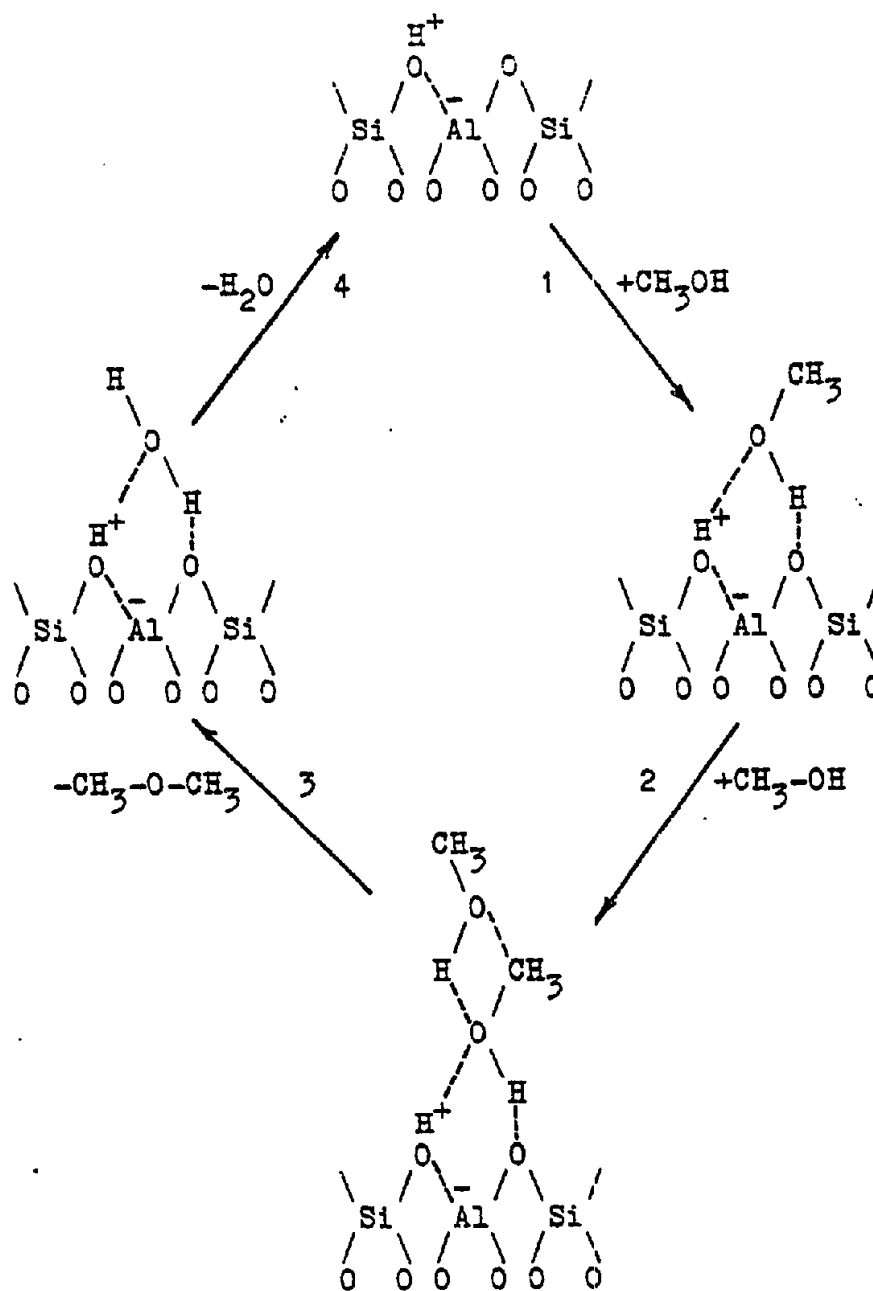
Figure 11. Formation of Dimethylether

$$CH_3-O-CH_3$$
$$+$$
$$H^+$$
$$\underline{\quad\quad O \quad\quad}$$

$$\longrightarrow$$

$$CH_3-OH$$
$$+$$
$$^+CH_3$$
$$\underline{\quad\quad O \quad\quad}$$

$$CH_3-O-CH_3$$
$$+$$
$$^+CH_3$$
$$\underline{\quad\quad O \quad\quad}$$

$$\longrightarrow$$

$$CH_3-OH$$
$$+$$
$$^+CH_2{\overset{\displaystyle CH_3}{\diagup}}$$
$$\underline{\quad\quad O \quad\quad}$$

$$^+CH_2{\overset{\displaystyle CH_3}{\diagup}}$$
$$\underline{\quad\quad O \quad\quad}$$

$$\longrightarrow$$

$$CH_2=CH_2$$
$$+$$
$$H^+$$
$$\underline{\quad\quad O \quad\quad}$$
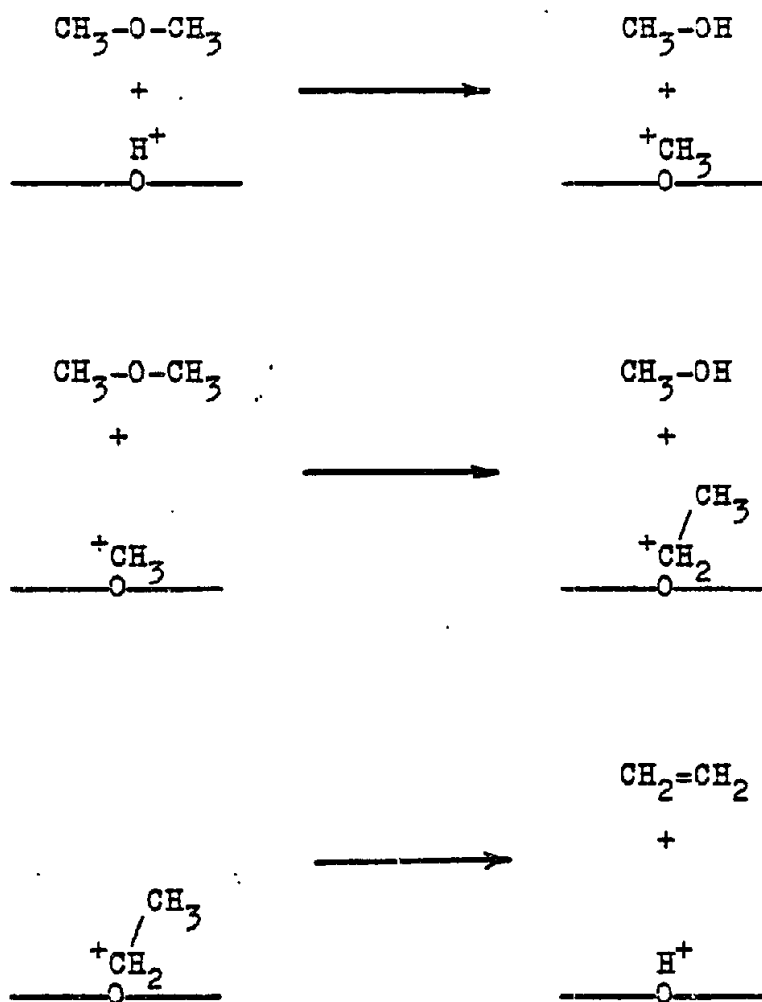
Figure 12.   Formation of Ethene

$CH_2=CH_2$

$+$

H^+

———O———

↓

$+CH_2 \underset{}{\overset{CH_3}{\diagup}}$

———O———

$+CH_2=CH_2$ ↙   ↘ $+CH_3-O-CH_3$

CH_3
$\diagup$
CH_2
$\diagup$
CH_2
$\diagup$
$+CH_2$

———O———

CH_3-OH

$+$

$_3HC \quad \overset{CH_3}{\diagup}$
$+CH$

———O———

↓

↓

$CH_2=CH-CH_2-CH_3$

$CH_2=CH-CH_3$

$\overset{+}{H^+}$

———O———

$\overset{+}{H^+}$

———O———
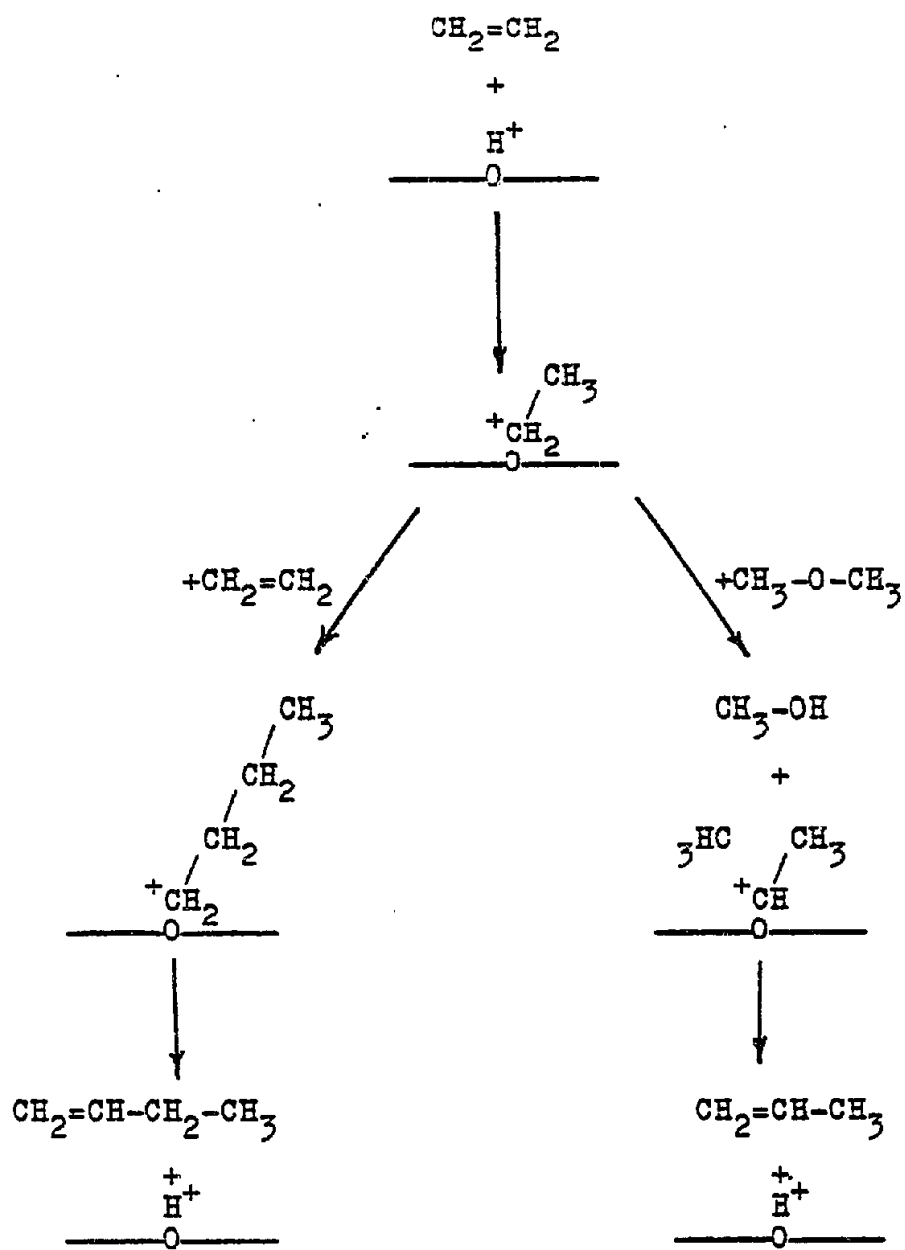
Figure 13. Formation of Higher Olefins

$$R_1-CH=CH-R_2$$

$$+$$

$$H^+$$
$$\underline{\quad\quad O \quad\quad}$$

$$R_3-CH_2-CH=CH-R_4$$

$$H^-$$

$$R_1-\overset{+}{CH}-CH_2-CH_2$$
$$\underline{\quad\quad O \quad\quad}$$

$$R_1-CH_2-CH_2-R_3$$

$$+$$

$$R_3-\overset{+}{CH}-CH=CH-R_4$$
$$\underline{\quad\quad O \quad\quad}$$
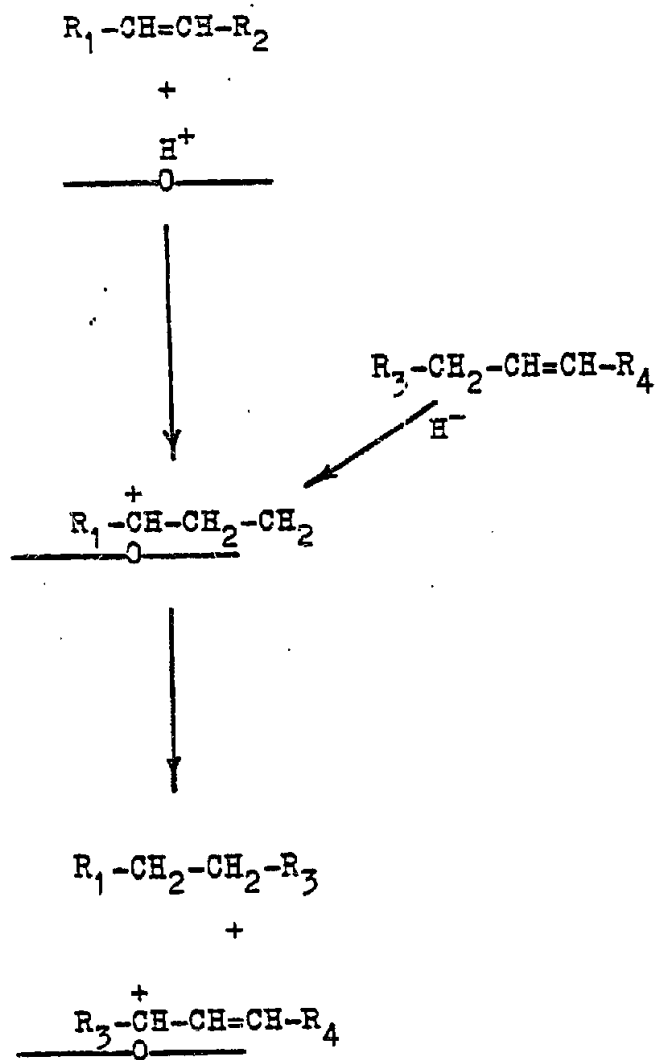
Figure 14. Formation of Paraffins

olfins and paraffins, respectively. Formation of paraffins was accomplished by hydride transfer from a larger olefin molecule to form a thermodynamically more stable smaller paraffin while leaving a hydrogen deficient surface hydrocarbon species. This hydrogen deficient species was speculated as the precursor to coke. Thus, formation of paraffins was accompanied by coke build-up. Catalytic testing results from the prepared catalysts showed no appreance of coke. This contradiction could be reconciled by recognizing that hydrogen generated by the water gas shift reaction was available to hydrogenate the coke precursor to paraffins.

It was reported by Singh (1980) that addition of water to the methanol feed increased olefin selectivity in the hydrocarbon product. Furthermore, experimental Run # Z6 to Z7 showed that presence of water substantially retarded the hydrogenation of ethylene. Based on these results and the proposed carbenium ion mechanism, the effect of water on paraffin formation may be explained in the following manner. Higher water partial pressure in the reaction mixture might caused an increase in the number of surface carbenium ions stablized by the presence of adjacent adsorbed water (Figure 15.). The stablized carbenium ion species was favored thermodynamically to desorb as ethylene rather than to further react with another gas phase olefin to form ethane by hydride abstraction while leaving a coke precursor on the

surface. Reduction of coke.precursor by the formation of a stablized carbenium ion species was in agreement with the generally known fact that water inhibits the formation of hydrogen deficient polymeric material on the surface of acidic catalyst.
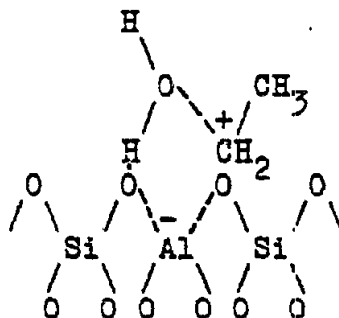
Figure 15.   Stablized Carbenium Ion

CHAPTER VII

X-RAY DIFFRACTION STUDIES

Qualitative characterization of the prepared catalysts were carried out using an x-ray powder diffraction technique in an effort to understand the effects of modification on the catalyst such as the incorperation of methanol synthesis component onto or into the zeolite matrix. Each prepared catalyst was studied using x-ray powder diffraction during each step of its preparation. The diffractometer which was used was the Diano XRD 800 with copper tube and nickel filter to obtain Cu K_α radiation. The operating conditions for the diffractometer were maintained constant for every sample, and the operating parameters were given in APPENDIX E. Petroleum jelly was used as the binding material in sample preparation. Background scarttering due to the binder was examined to be minimal. Identification of a compound was made using published d-spacing values. Published x-ray data for erionite and zinc-copper oxide were given by Breck (1974) and "Powder Diffraction File Search Manual" (1973), respectively. Crystallinity of the zeolite matrix was qualitatively examined by comparing the intensity and sharpness of the reflection peaks from zeolite to the broad scartering background from amorphous aluminosilicate.

Commercial high pressure methanol synthesis catalyst, zinc chromite, was examined using powder diffraction

technique to be containing zinc oxide, Figure 16.
Diffraction pattern for sodium erionite and rare earth and
ammonium chloride exchanged erionite was given in Figure 17
and 18, respectively, and the patterns showed that no
degradation of the zeolite matrix occurred during the ion
exchange process. Diffraction pattern for the commercial
adsorbent Zeolon-500, a mixture of erionite and chabazite,
was given in Figure 19, and it showed that the crystallinity
of the zeolite mixture was relatively low compared to
erionite, Figure 18, obtained from Union Carbide. Figures
20 and 21 were the diffraction patterns for prepared
catalyst Cat. 1 before and after catalytic tests,
respectively, and the diffraction patterns indicated no
substantial reduction of crystallinity occurred during the
catalytic tests. Identification of the zinc oxide phase was
not performed because of the uncertainty introduced by the
broad scartering of the amorphous phase. However, the
diffraction patterns of Cat. 1 showed no increase in
amorphous material which indicated the lack of coke build-up
in the zeolite matrix during the catalytic tests.
Diffraction patterns for prepared catalyst Cat. 2 before and
after calcination process are given in Figure 22 and 23,
respectively. Predominant change of the prepared catalyst
Cat. 2 during calcination process was an increase of
crystallinity in the zinc oxide phase which might have been
caused by the sintering of the zinc oxide crystallite. But,

p
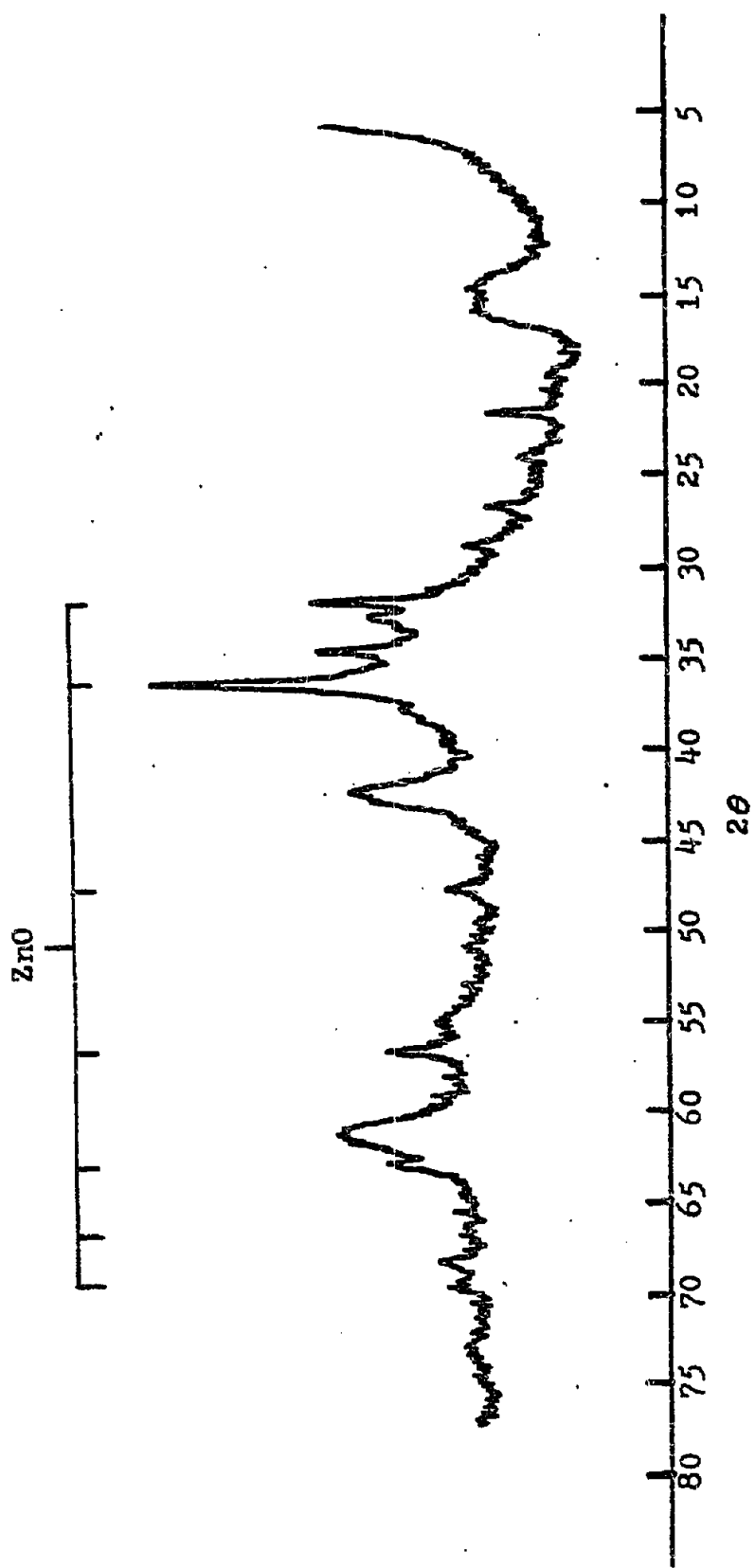
Figure 16. Diffraction Pattern for Zinc Chromite
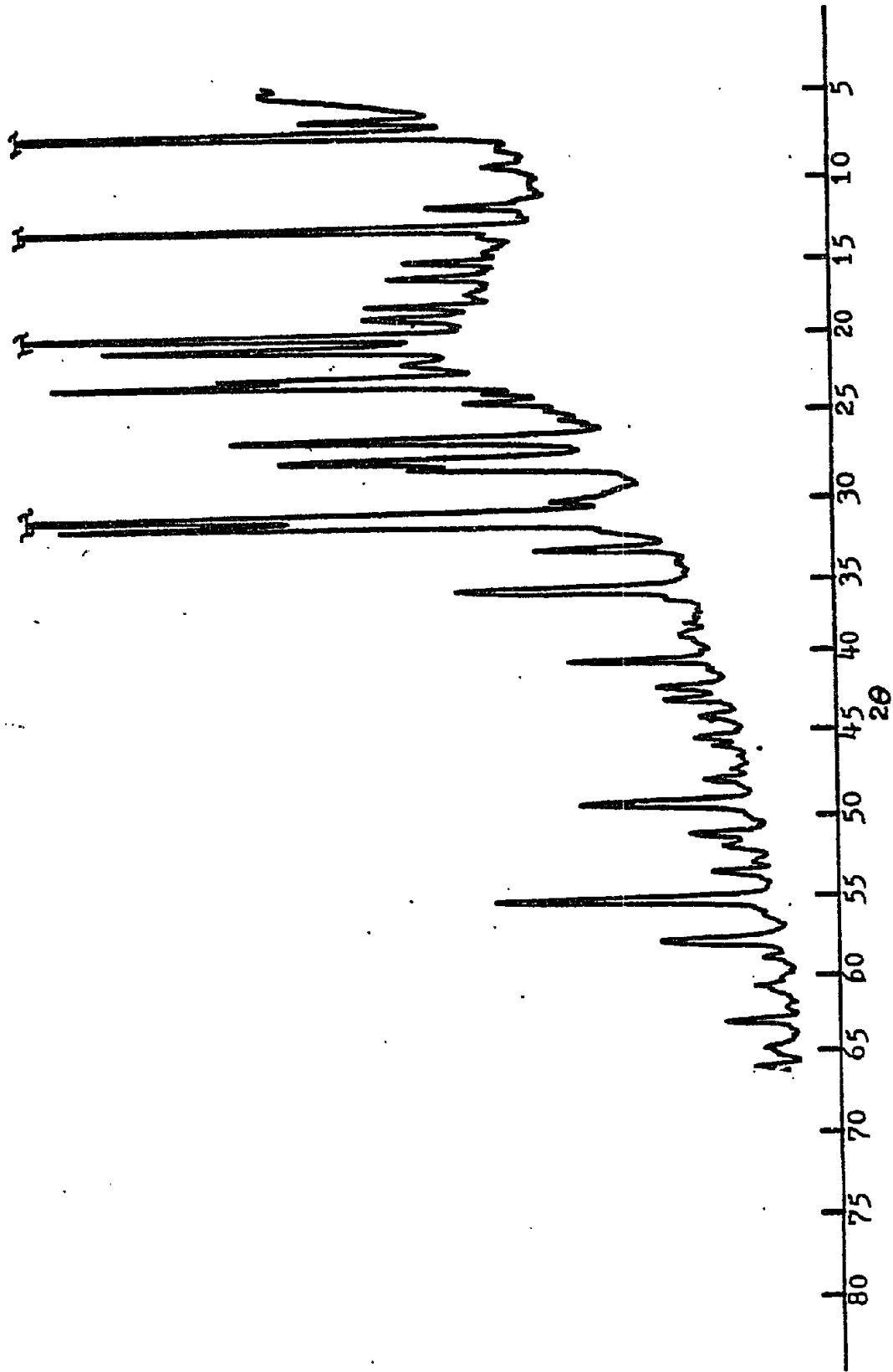
Figure 17: Diffraction Pattern for Na-Erionite
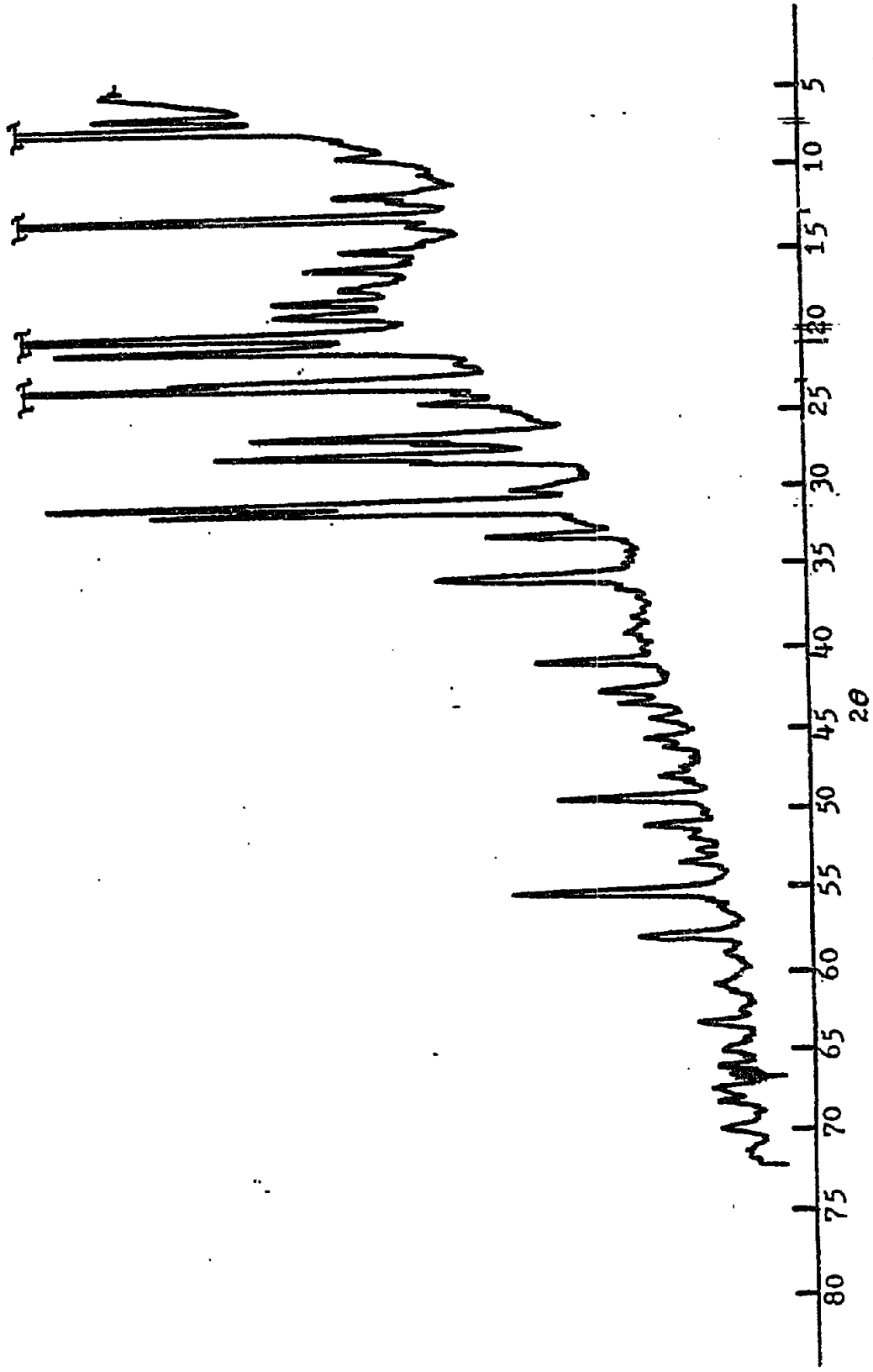
Figure 18. Diffraction Pattern for Ammonium and Rare Earth Exchange Erionite

2θ
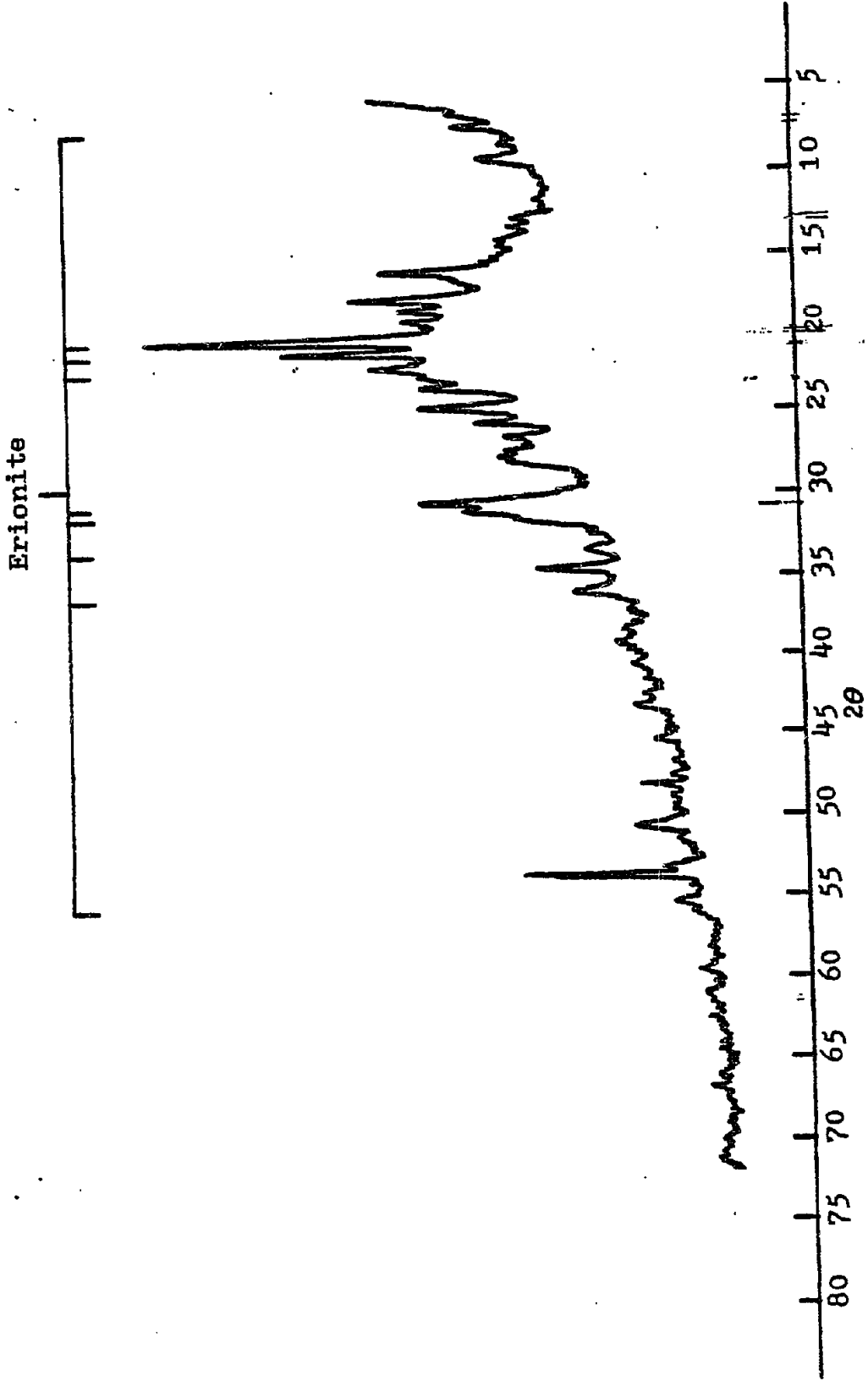
Figure 19.   Diffraction Pattern for Zeplon 500
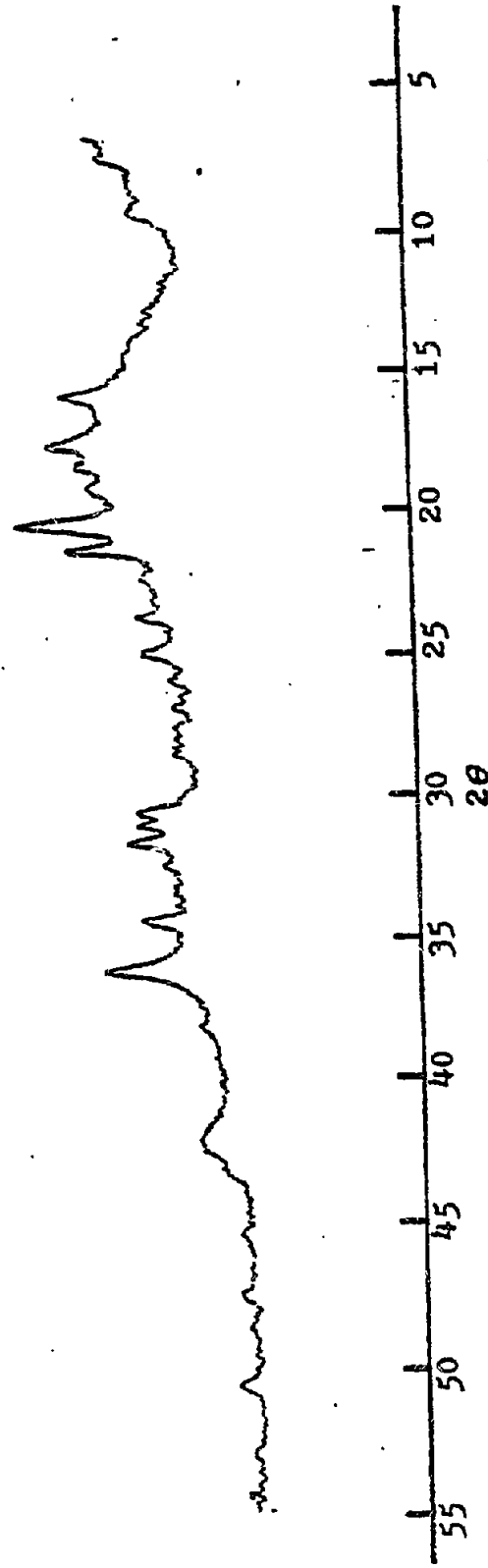
Figure 20. Diffraction Pattern for Cat. 1 before Reaction

p
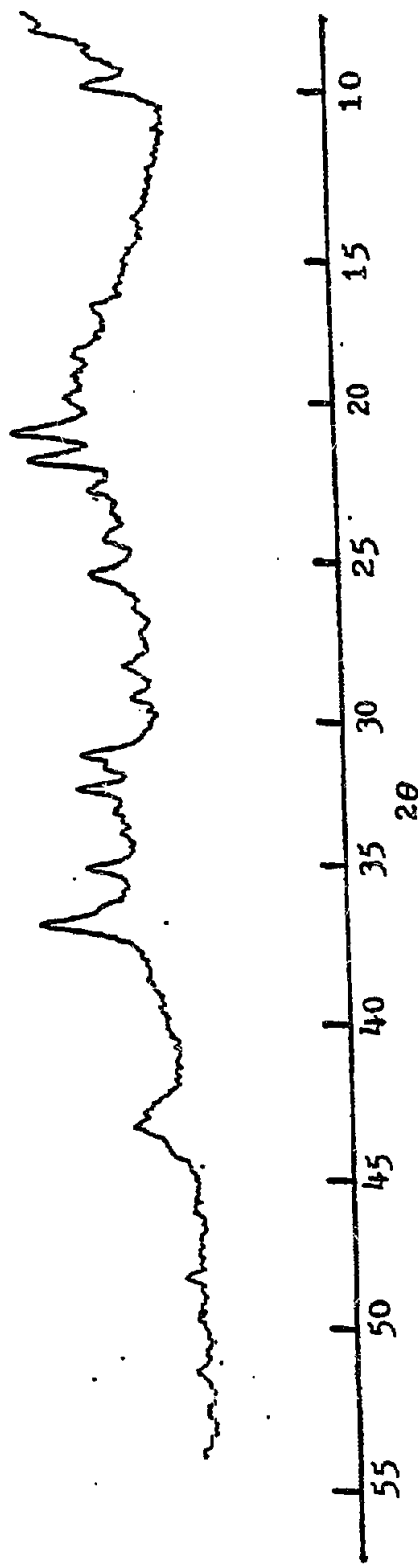
Figure 21. Diffraction Pattern for Cat. 1 after Reaction
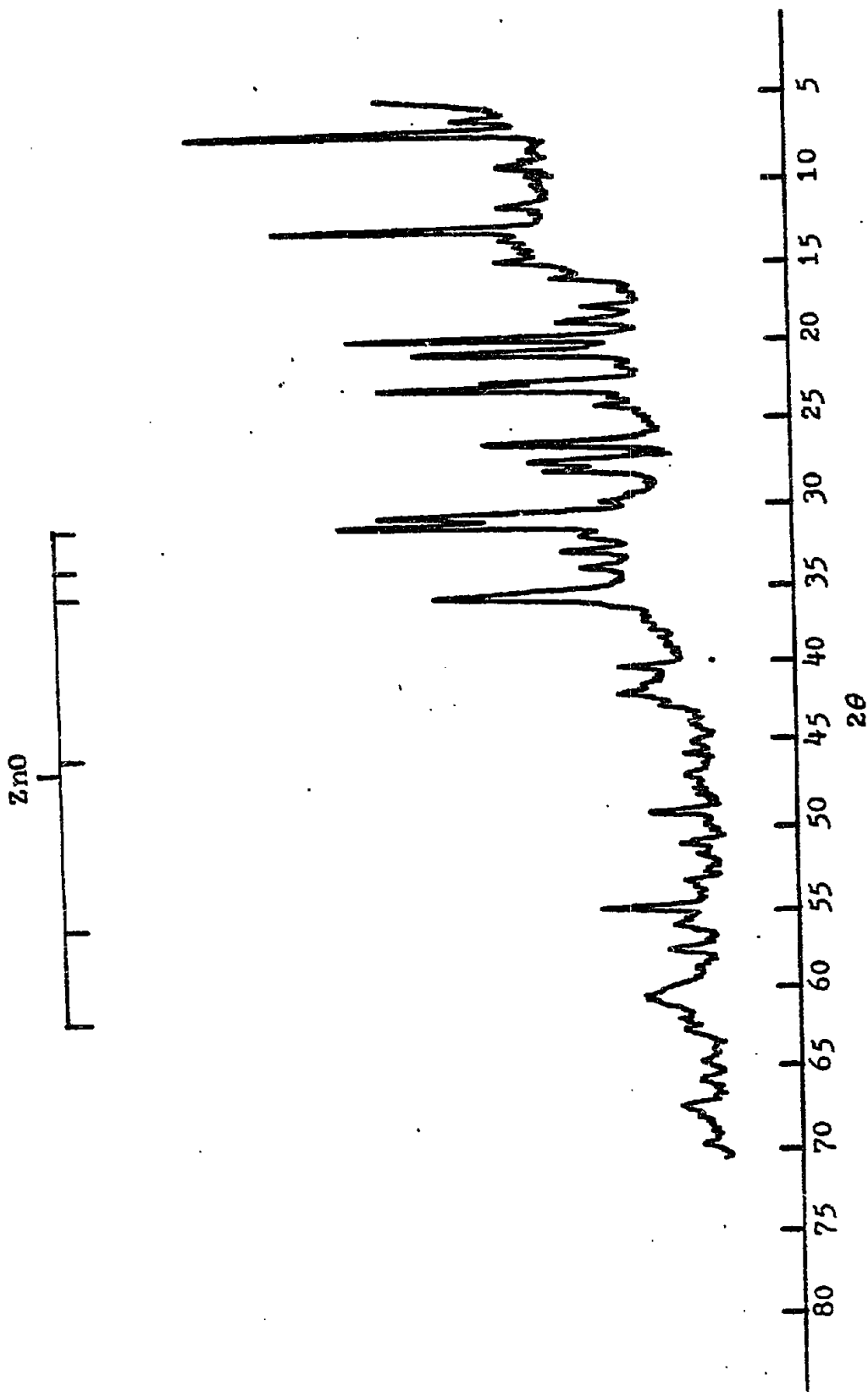
Figure 22. Diffraction Pattern for Cat. 2 before Calcination
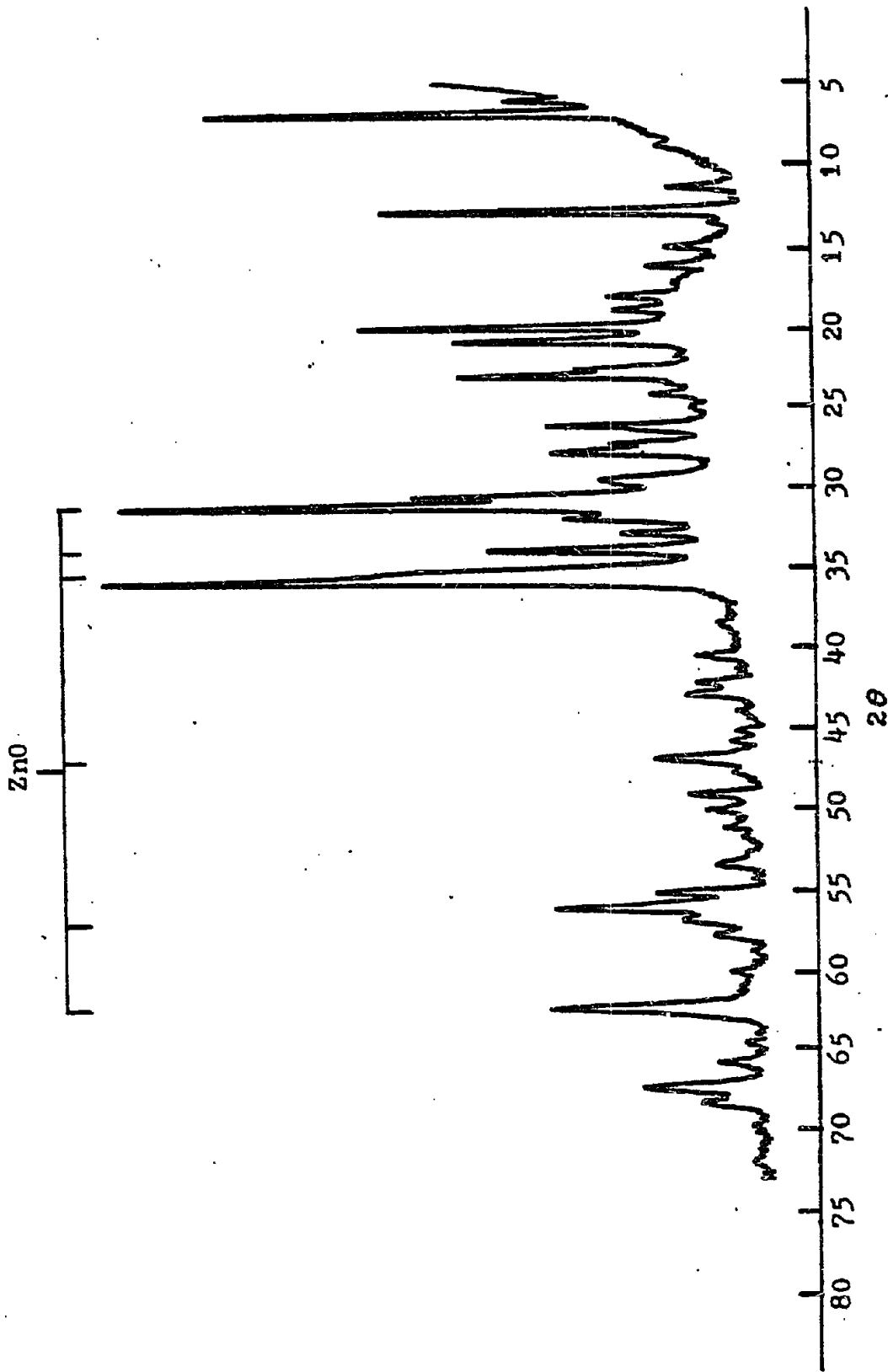
Figure 23. Diffraction Pattern for Cat. 2 after Calcination

no substantial changes occurred in the structure of Cat. 2
during catalytic testings, as indicated in Figure 23 and 24.
Diffraction patterns for prepared catalysts Cat. 3 and Cat.
4 before and after catalytic testing period were presented
in Figures 25, 26, 27, and 28, respectively. Identification
of the zinc oxide phase in prepared catalysts Cat. 3 and
Cat. 4 was not performed due to the low oxide loading level.
The diffraction patterns of Cat. 3 and Cat. 4 both showed a
substantial loss of crystallinity in the zeolite matrix
before the catalytic tests. The loss of crystallinity in
the zeolite matrix might have been caused by the excessive
steam stripping of the zeolite matrix aided by decomposition
of metal nitrate during the calcination process. However
both Cat. 3 and Cat. 4 still showed catalytic activities and
selectivities for C_1 to C_4 hydrocarbon production as shown
in Figure 10. The catalytic activities and selectivities of
the partially stripped catalysts could be contributed to the
high activity of the remaining zeolite. Figures 29 and 30
were the diffraction patterns for prepared catalyst Cat. 5
before and after catalytic tests, respectively. The main
feature in the structural changes of the catalyst affected
by the catalytic tests was the appearance of copper metal.
The copper or zinc oxide phase was unable to be detected
because of the low loading level and line broadening by the
remaining oxide crystallite. However, line broadening by
crystallite can be considered as an indicator of the
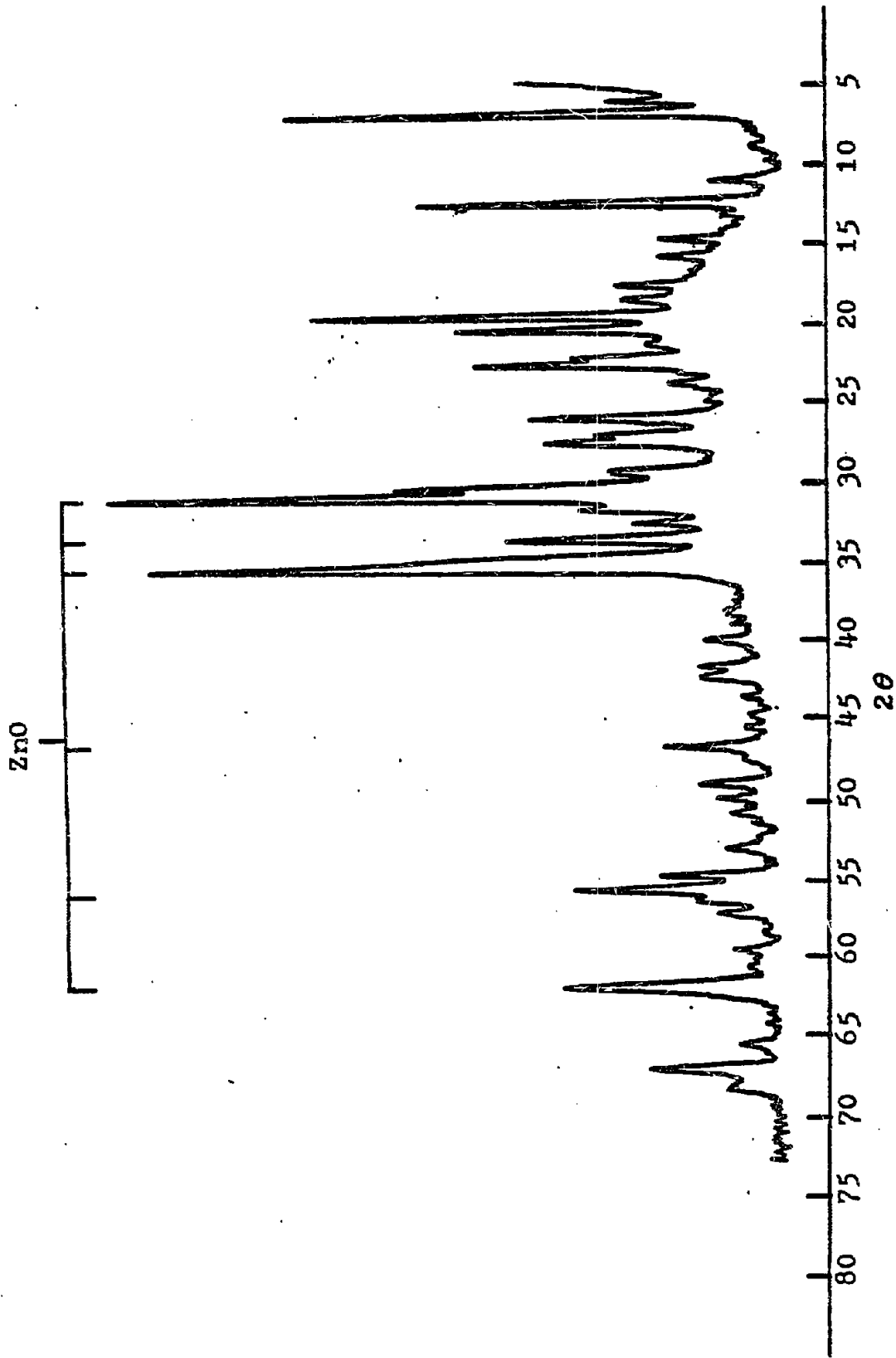
Figure 24. Diffraction Pattern for Cat. 2 after Reaction
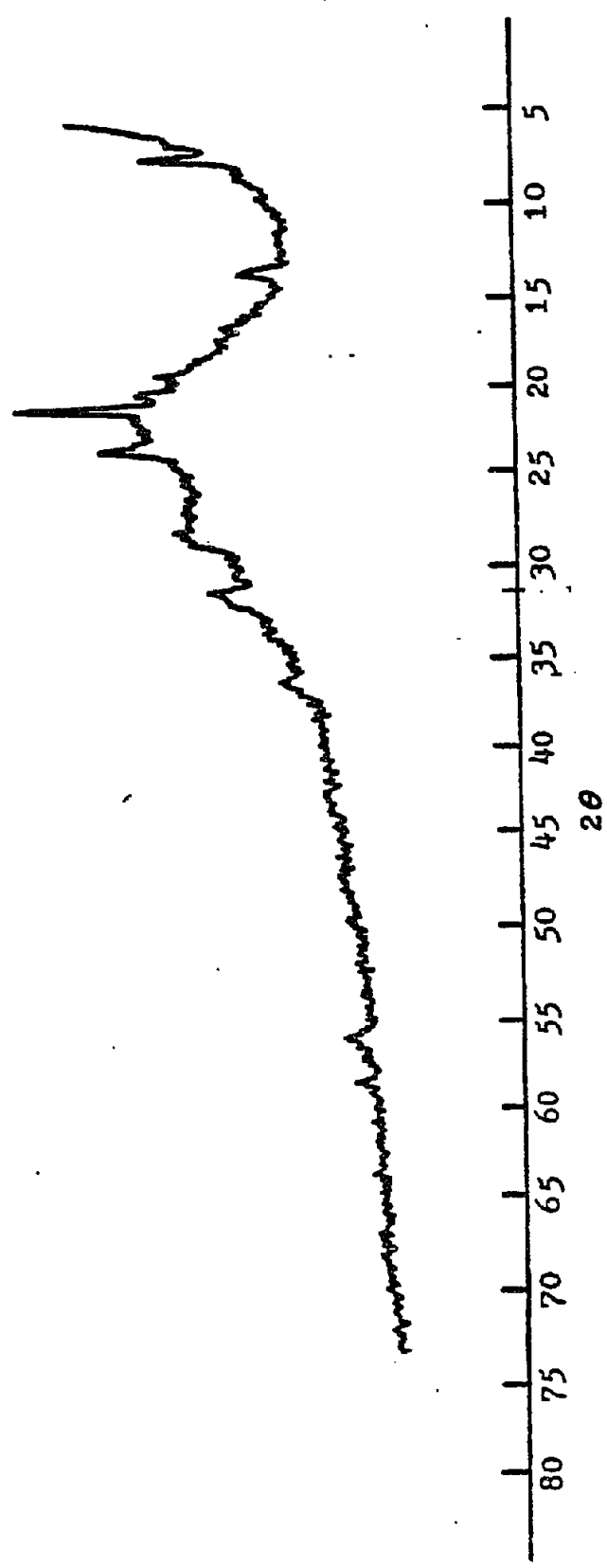
Figure 25. Diffraction Pattern for Cat. ‖ before Reaction
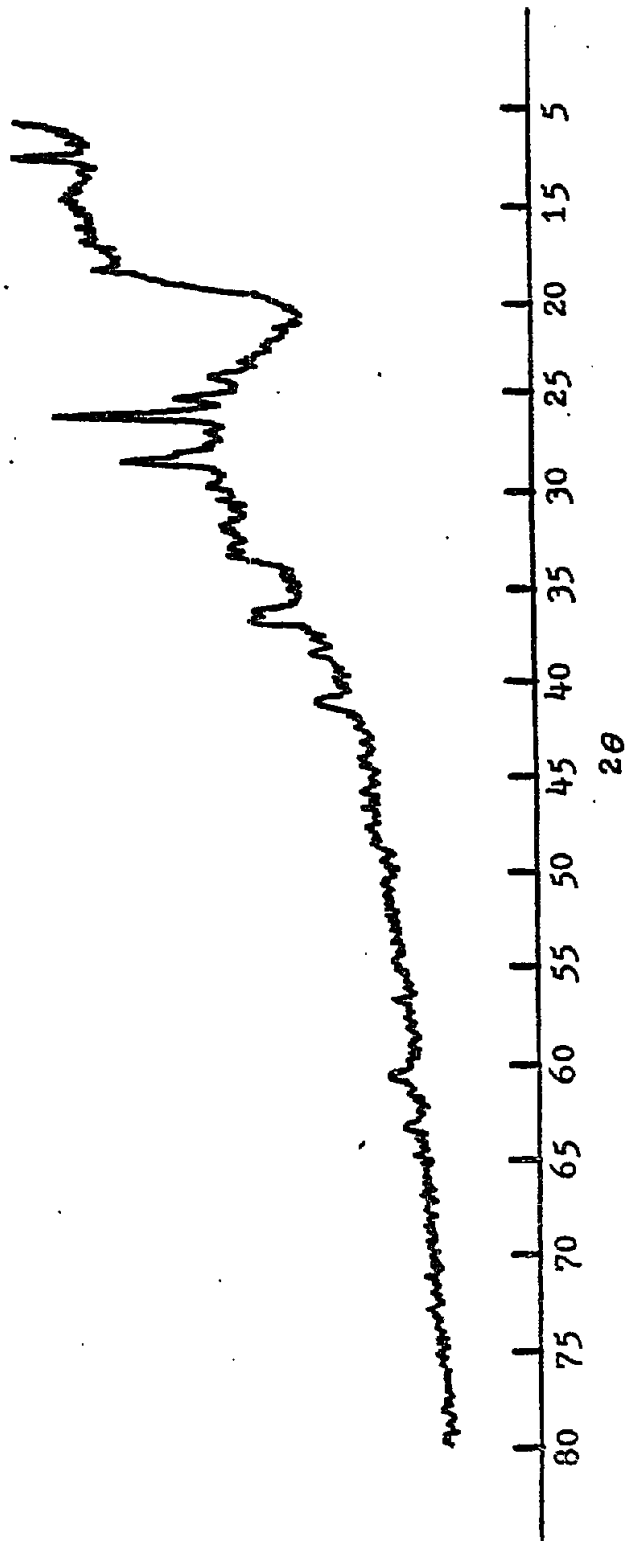
Figure 26. Diffraction Pattern for Cat. 3 after Reaction
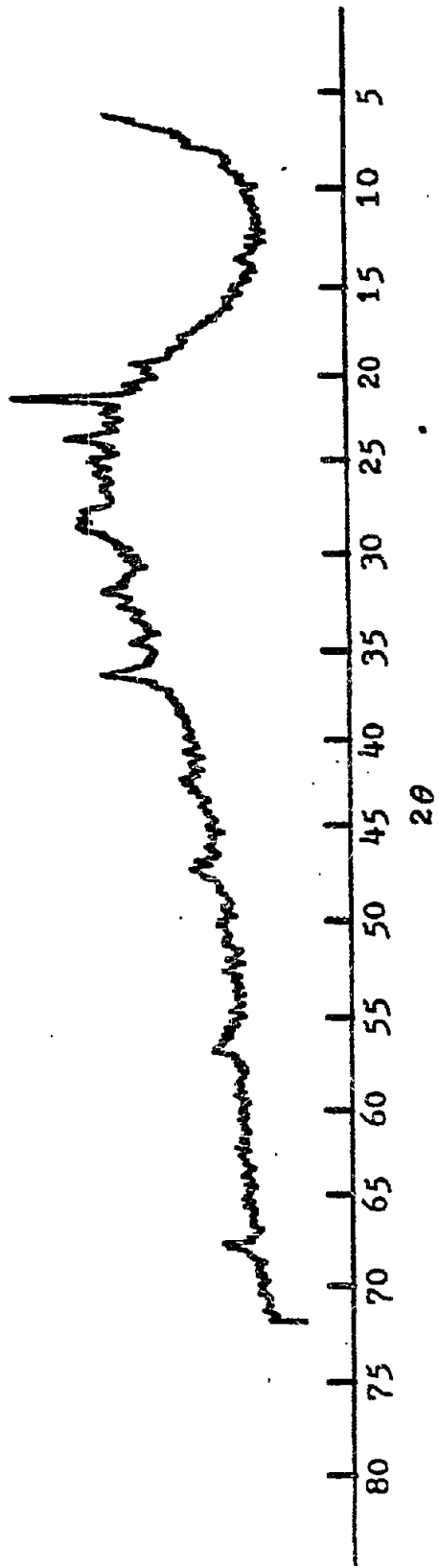
Figure 27. Diffraction Pattern for Cat. 4 before Reaction
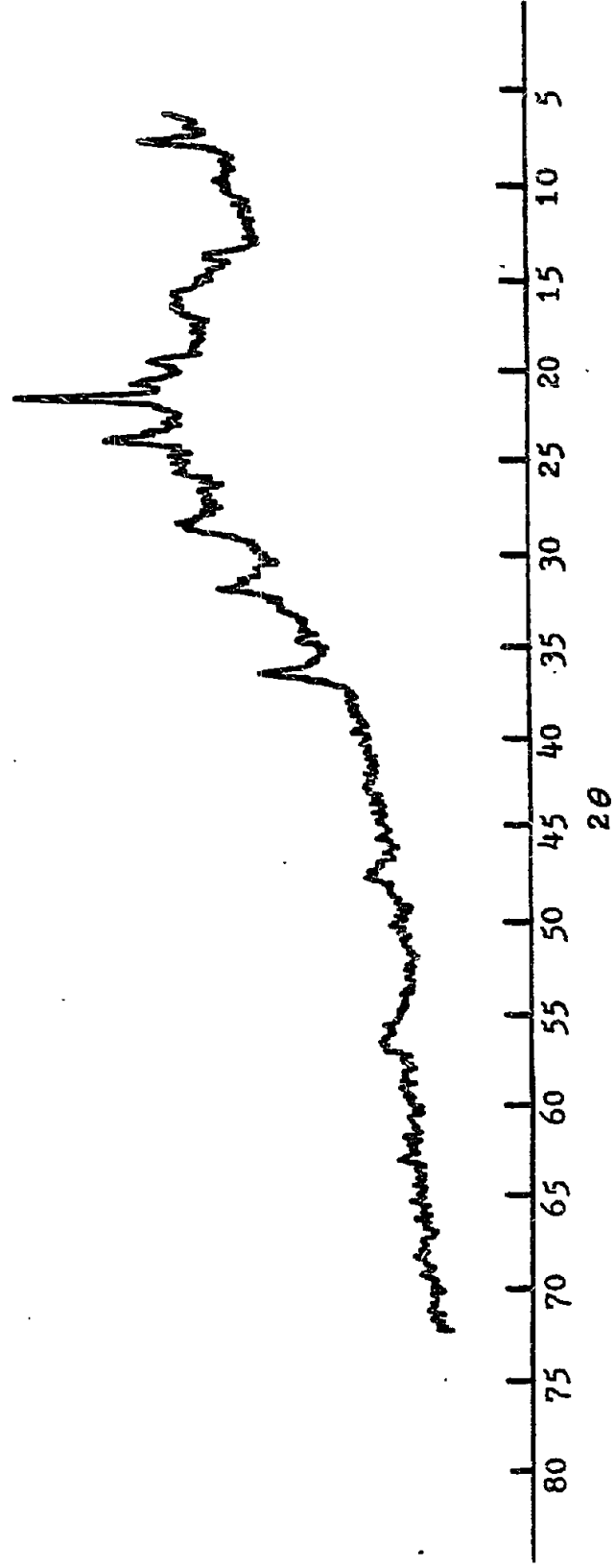
Figure 28. Diffraction Pattern for Cat. 4 after Reaction
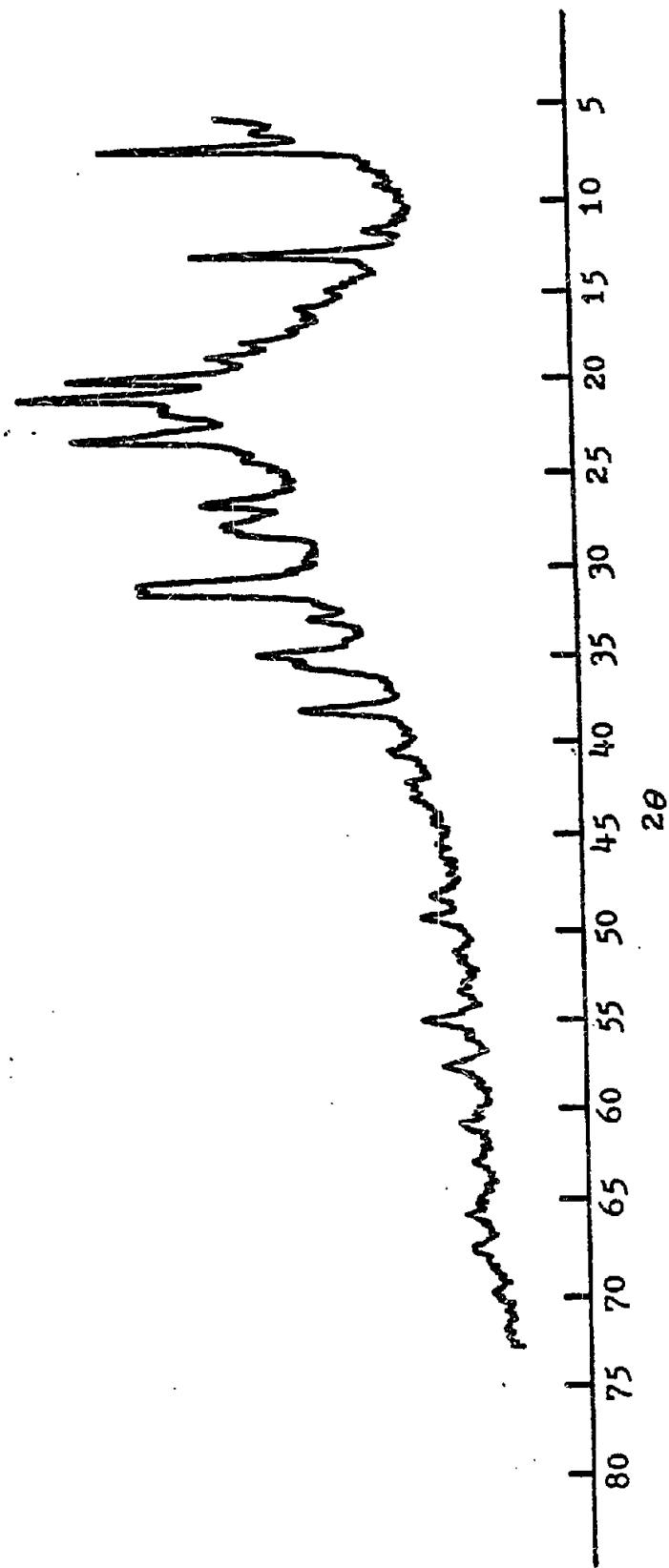
Figure 29. Diffraction Pattern for Cat. 5 before Reaction
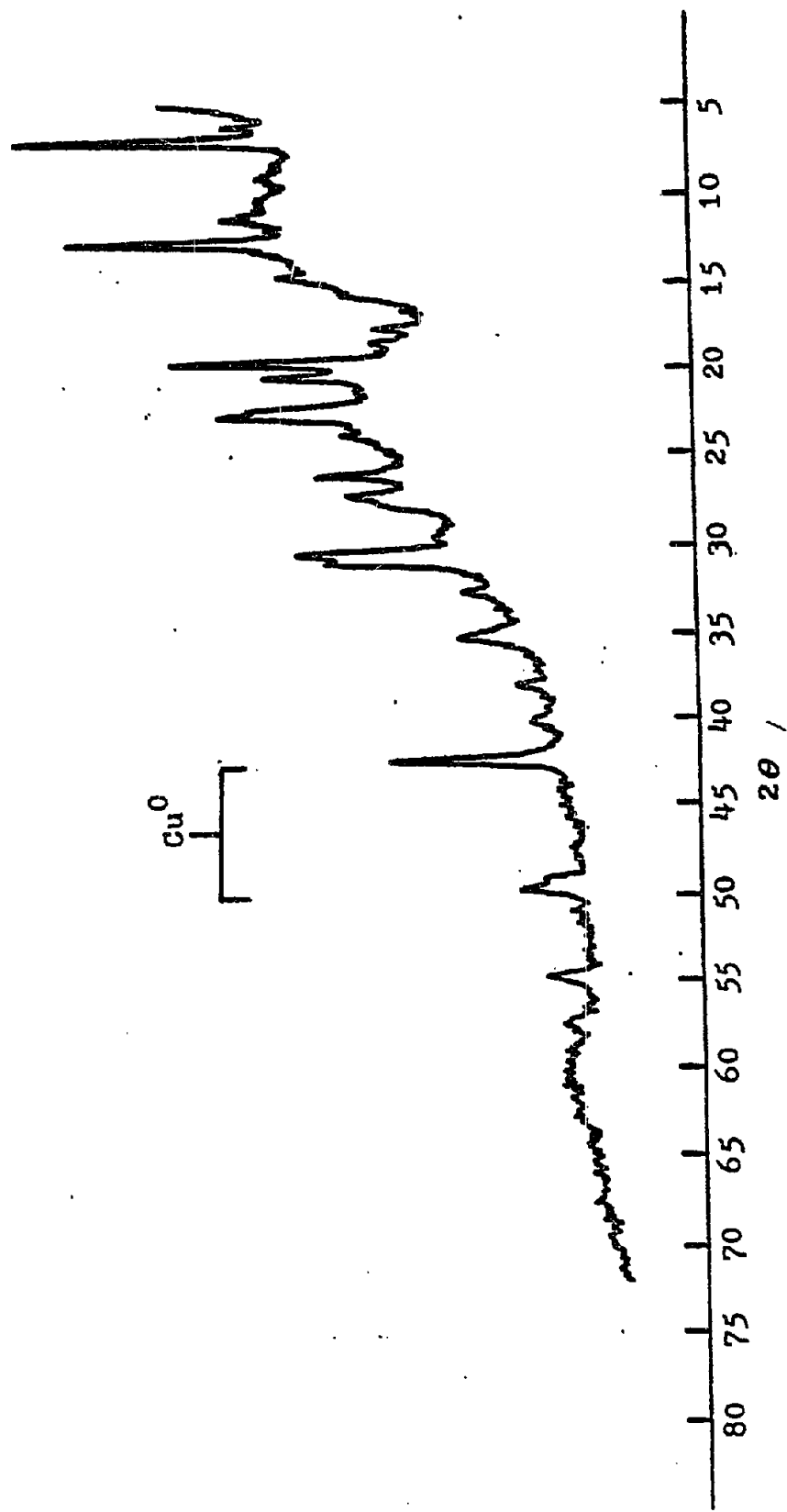
Figure 30. Diffraction Pattern for Cat. 5 after Reaction

efficiency in the impregnation technique. Figures 31 and 32 were the diffraction patterns for prepared catalyst Cat. 6 before and after calcination, respectively. The most noticeable change was the conversion of $(Cu,Zn)_2(OH)_2CO_3$ preciptate to the oxide form with the zeolite structure unchanged. The appearance of copper metal was detected in the diffraction pattern of prepared catalyst Cat. 6 after catalytic tests, Figure 33. The copper metal was formed by the reduction of copper oxide with synthesis gas during the reaction. However, the zinc oxide and the zeolite phase were unchanged , and the reduction of the copper oxide was incomplete in which copper oxide was still detected after the initial reduction.

The conclusions of the x-ray powder diffraction studies were the following:

1 Coke was not observed.

2 Ion exchange process had no structural effect

3 Metal nitrate decomposition had a substantial degradation on the zeolite component.

4 Copper oxide as a part of the methanol synthesis catalyst was not completely reduced, and the methanol synthesis function was retained.
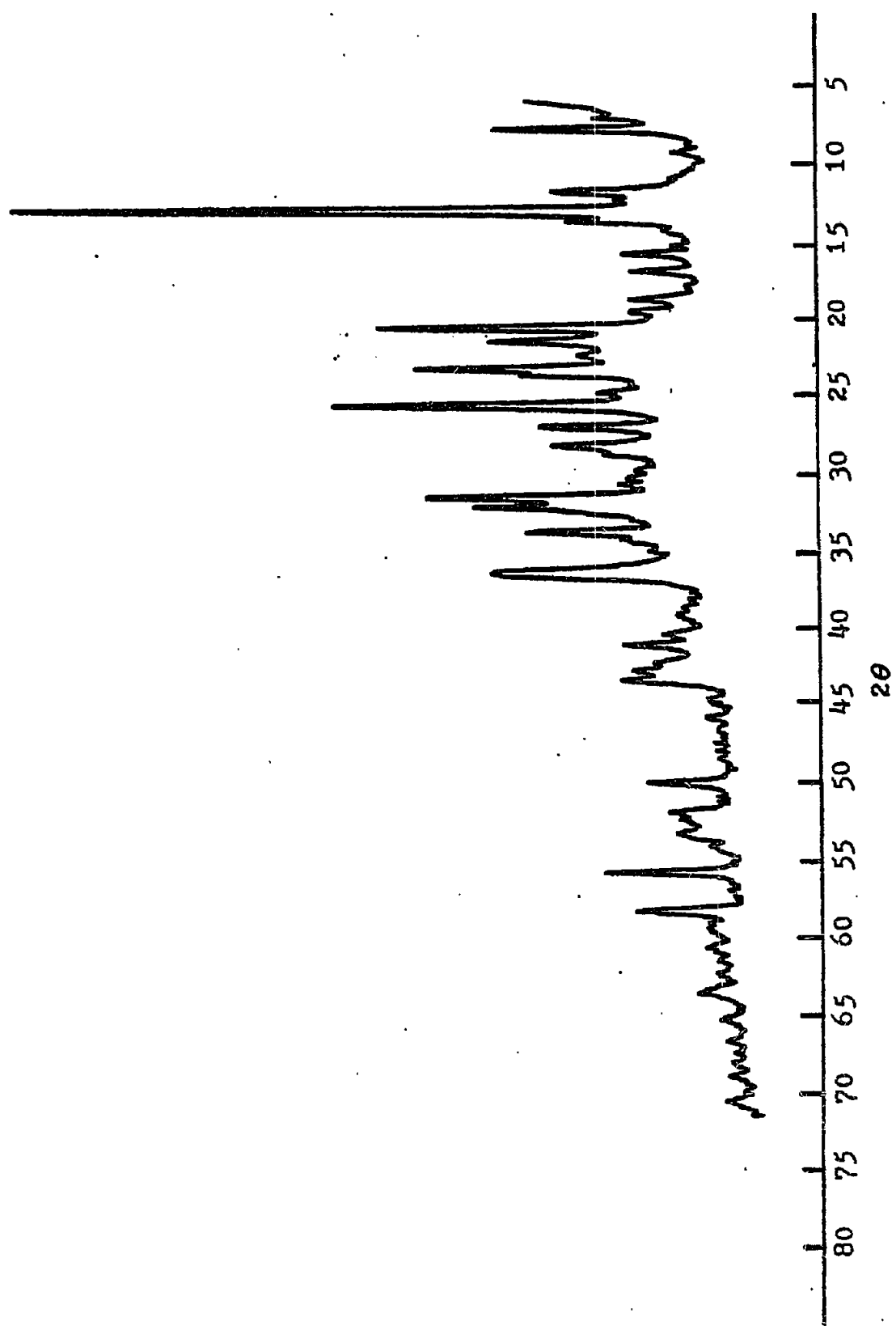
Figure 31. Diffraction Pattern for Cat. 6 before Calcination
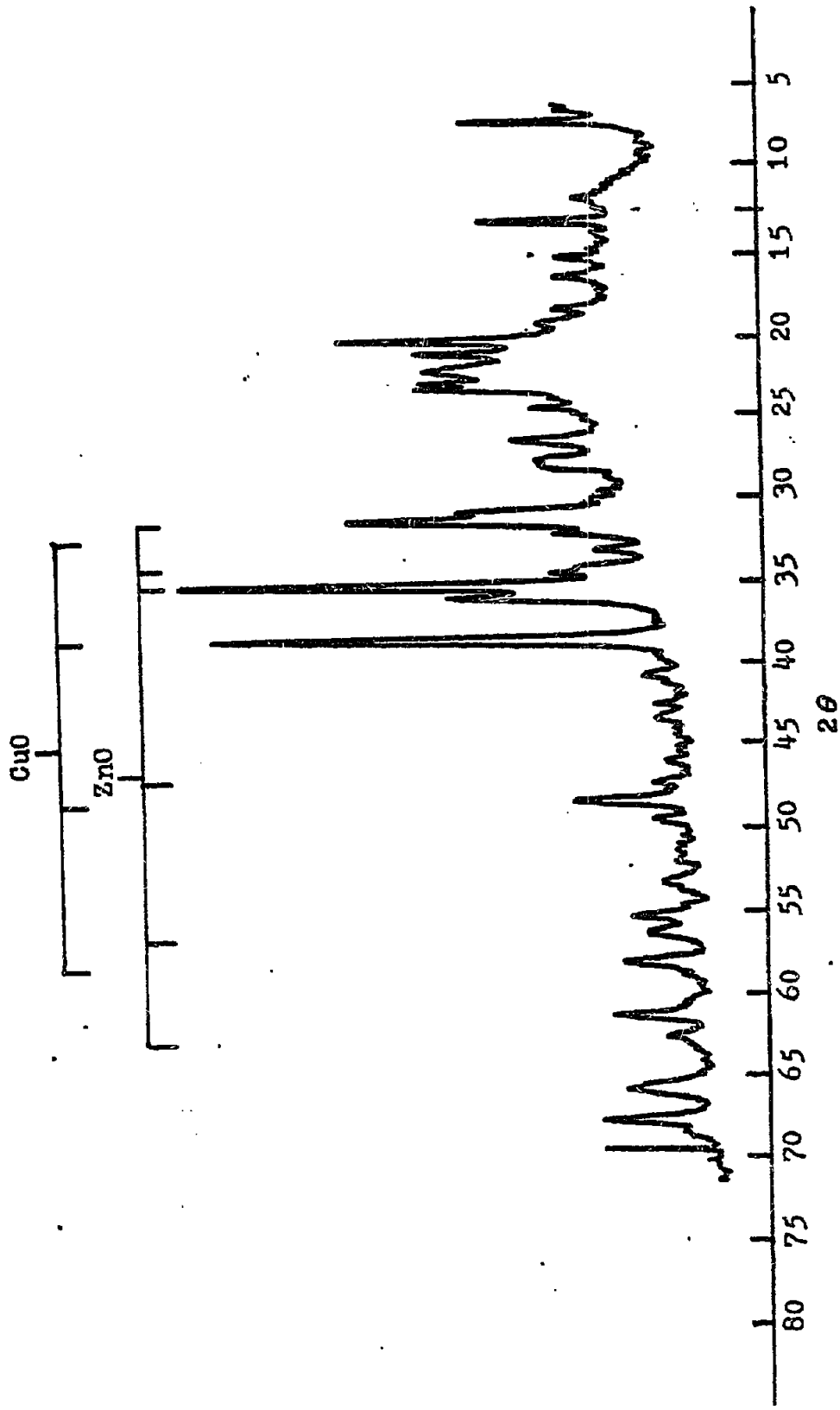
Figure 32. Diffraction Pattern for Cat. 6 after Calcination
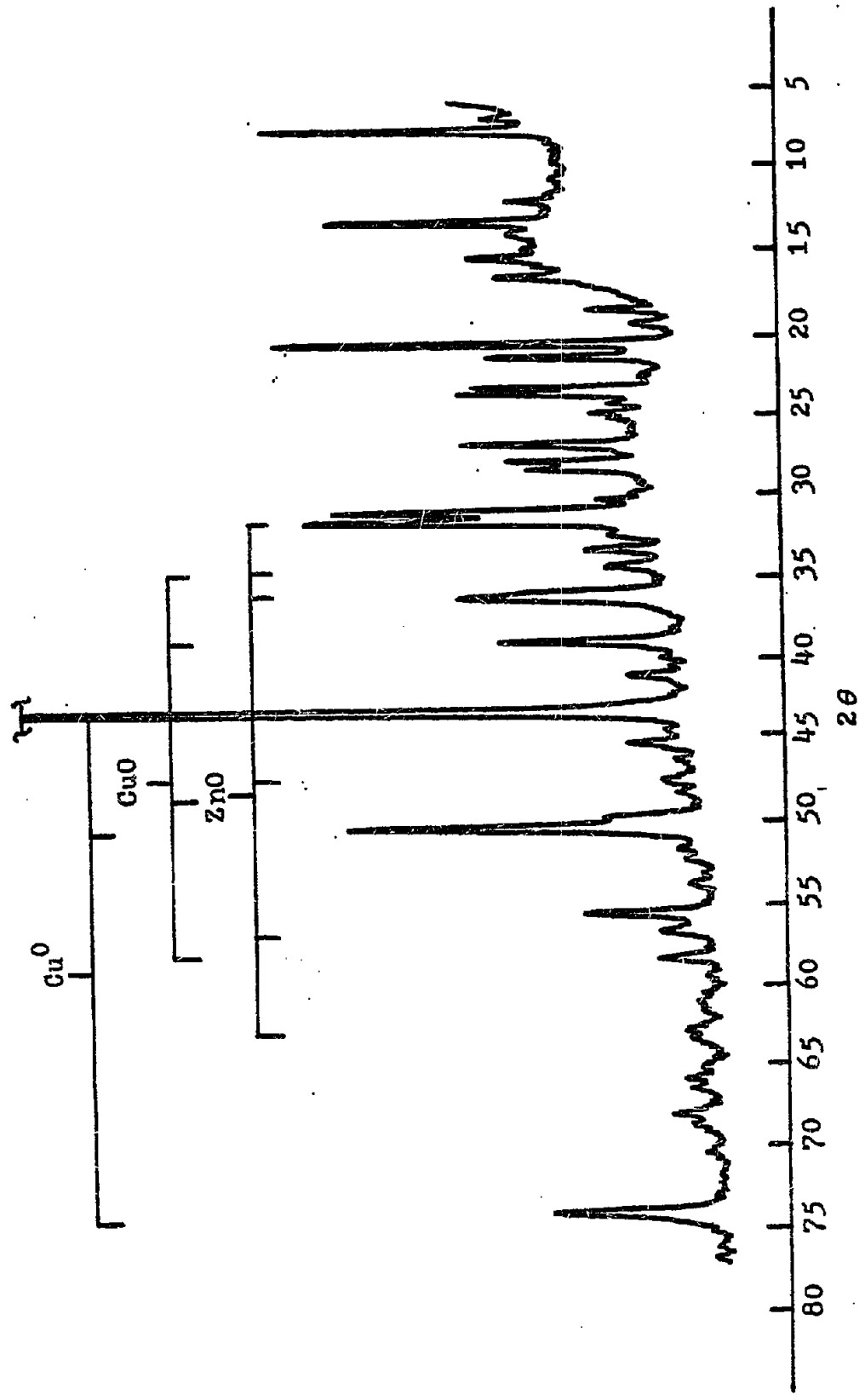
Figure 33. Diffraction Pattern for Cat. 6 after Reaction

CHAPTER VIII

CONCLUSIONS AND RECOMMENDATIONS

The object of this thesis was to develop and study a set of non-trivial bifunctional catalysts which can selectively convert synthesis gas to low molecular weight hydrocarbons. A total of six catalysts were prepared and tested using three different methods of preparation. Rare earth and ammonium chloride exchanged erionite was used as the methanol decomposition to hydrocarbon catalyst, and zinc oxide and mixed copper and zinc oxide were used as the methanol synthesis catalyst.

Catalytic testing results showed that methanol and hydrocarbons were produced which indicated that the catalyst component was active and cooperative in synthesis gas conversion to hydrocarbons. The hydrocarbons produced were in the C_1 to C_4 hydrocarbon range. The sharp carbon distribution of the hydrocarbon products showed the shape selectivity of the zeolite component catalyst, erionite. Paraffinic content of the hydrocarbon product fraction was high compared to the olefinic content. Experiments on ethylene hydrogenation showed that both methanol synthesis and zeolite catalyst component were active in olefin hydrogenation. Thus, the high paraffinic content of the hydrocarbon products was the result of hydrogenation of olefinic intermediate products. However, it was found that

water had a retarding effect on ethylene hydrogenation over zeolite catalyst component. In view of the retarding effect by water on olefin hydrogenation and the generally accepted fact that olefin was the primary product of methanol conversion to hydrocarbons, the author of this study speculated that a stablized surface carbenium ion species was a thermodynamically more favorable surface precusor to ethylene in an excess water environment. All of the prepared catalysts exhibited catalytic activity for the water gas shift reaction, and the testing results showed that the extent of the water gas shift reaction was in dynamic equilibrium. This result was in agreement with the generally known fact that the methanol synthesis catalyst component was a good shift catalyst.

X-Ray diffraction studies on the prepared catalysts showed that coke was not formed during the reaction. The study showed that ion exchange process had no structural effect on the zeolite matrix. Metal nitrate decomposition over the zeolite component had a substantial degradation effect on the crystallinity of the zeolite matrix. However, the degradation of the zeolite matrix was not complete in that the remaining zeolite matrix still exhibited high activity and selectivity for hydrocarbon production. Copper oxide as a part of the methanol synthesis catalyst was partially converted to copper metal, but the remaining mixed oxide was shown to retain much of its catalytic activity in

methanol synthesis.

Based on the reults of this study and literature review, the following recommendations were suggested for further investigation.

1. A catalytic study on olefin hydrogenation over methanol synthesis catalyst was needed to understand the nature of olefin hydrogenation on a methanol synthesis catalyst. This study was aimed for possible reduction of olefin hydrogenation over methanol synthesis catalyst.

2. Effect of water on olefin hydrogenation over zeolite catalyst needed to be investigated.

3. A study on acid strength distribution of the catalytic active acid site was needed to control the methanol decomposition to hydrocarbons.

4. ^{18}O Tracer study on the methanol synthesis catalyst was needed to determine the role played the lattice oxygen.

5. Experiments using other small pore zeolite such as mordenite as the zeolite component was needed to understand the effect of zeolite geometry and acidity on hydrocarbon distribution.

LITERATURE CITED

Badische Amilin-und Soda Fabrick, German Patents: 295203
and 295204 (1913)

Baird, M. J., Schehl, R. R., and Haynes, W. P., "Fischer-
Tropsch Process Investigated at the Pittsburgh Energy
Technology Center Since 1944," U.S. Dept. of Energy,
Technical Review (1977)

Berty, J. M., "Reactor for Vapor-Phase Catalytic Studies,"
Chem. Eng. Prog., **70**, 79 (1974)

Breck, J. M., Zeolite Molecular Sieves, John Wiley & Son,
New York (1974)

Editors, "Key Chemicals, Methanol," Ch. & Eng. News,
Jan. 22, **13**, (1979)

Chang, C. D., Lang, W. H., and Silvestri, A. J.,
"The Conversion of Methanol and Other O-Compounds to
Hydrocarbons over Zeolite Catalysts," J. of Catal.,
56, 268 (1979)

Dietz, W. A., "Response Factors for Gas Chromatographic
Analyses," J. of Gas Chrom., **69**, 201 (1967)

Eischens, R. and Pliskin, W. A., "Infrared Spectra of
Adsorbed Molecules," Adv. Catalysis, **10**, 1 (1958)

Frohning, C. D. and Cornils, "Chemical Feedstock from
Coal," Hydro. Proc., **53**, 143 (1974)

Herman, R. G., Klier, K., Simmons, J. K., Finn, B. P.,
Bulko, J. B., and Kobylinski, T. P., "Properties of
Methanol Catalysts," J. of Catal., **56**, 407 (1979)

Jacobs, P. A., Carboniogenous Activity of Zeolite,
Elsevier, Amsterdam (1977)

Kung, H. H., "Methanol Synthesis," Catal. Rev.-Sci. Eng., 22, 235 (1980)

Lin, F. N., Chao, J. C., and Anthony, R. G., "Conversion of Coal Based Methanol to Ethylene," Coal Processing Technology, Vol. IV, CEP, 73 (1978)

Mattox, W. J., U. S. Patent 33036134 (1962)

Nagarjunan, T. S., Sastri, M. V. C., and Kuriacose, "Simultaneous Adsorption of Hydrogen and Carbon Monoxide on Zinc Oxide," J. of Catal., 2, 223 (1963)

Natta, G., "Synthesis of Methanol," in Catalysis, Vol.III, ed. by P. H. Emmett, Reinhold Publ. Corp., 349 (1955)

Pichler, H. and Kruger, G., Herstellung flussiger Kraftstoffe aus Kohle, Gersbach & Sohn, Munchen (1973)

"Powder Diffraction File Search Manual-Inorganic (Fink Method)," Joint Committee on Powder Diffraction Standard, Swarthmore, Penn. (1973)

Rozorskii, A. Y., Kagan, Y. B., Lin, G. I., Slivinskii, E. V., Loktev, S. M., Libeerov, L. G., and Bashkirov, A. N., "Mechanism for the Synthesis of Methanol from Carbon Monoxide and Hydrogen," Kinet. Catal., 16, 706 (1975)

Salvador, P. and Kladnig, W., "Surface Reactivity of Zeolite Type H-Y and Na-Y with Methanol," V. C. S. Fraday Trans. I, 1153 (1977)

Singh, B. B., "Catalytic Conversion of Methanol to Low Molecular Weight Hydrocarbons," Doctor of Philosophy Dissertation, Texas A&M University (1980)

APPENDIX A

CATALYTIC TESTING DATA

The experimental data from the catalytic tests were tabulated in TABLE 3. Composition of the reaction effluent was expressed as molar precentage, and calculation procedure used to obtain the composition was given in APPENDIX C. The activity of the tested catalyst was expressed as molar conversion of carbon monoxide , and the calculation procedure used was presented in APPENDIX D. Equilibrium constant value for the water gas shift reaction was calculated using the procedure given in APPENDIX E. The following nomenclature was used in TABLE 3:

TOS (hr.)	:	Time on Stream
WHSV (hr.$^{-1}$)	:	Weight Hourly Space Velocity
Temp. (K)	:	Reaction Temperature
P (psig)	:	Reaction Pressure
X%	:	Molar Conversion of Carbon Monoxide in the Feed
*X%	:	Total Molar Conversion of Carbon in the Feed
*Kw	:	Theoretical Equilibrium Constant for the Water Gas Shift Reaction
Kw	:	Experimental Equilibrium Constant for the Water Gas Shift Reaction
Carbon Yield (%)	:	Molar Carbon Percentage of Compound i in the Product per Carbon Reacted

TABLE 3 CATALYTIC TESTING DATA

Date : 8-15-'80

Catalyst : Cat. 1

Feed : $CO:H_2$ (33.78 : 66.22)

History : Fresh

Product Composition (mole percent)

Run #	TOS hr.	WHSV hr.$^{-1}$	Temp. K	P psig	X%	H_2	CO	CO_2	H_2O	CH_4	C_2H_4	C_2H_6	C_3H_6	C_3H_8	C_4H_{10}	CH_3OH	DME
1.1	0.5	9.52	708	800	15.3	64.4	30.1	2.81	0.84	1.37	0.00	0.01	0.01	0.13	0.00	0.00	0.04
1.2	1.00	9.52	708	800	18.9	64.3	29.2	3.44	0.92	1.37	0.03	0.38	0.03	0.27	0.00	0.00	0.07
1.3	1.50	9.52	708	800	20.9	64.5	28.7	3.74	0.91	1.15	0.07	0.35	0.08	0.42	0.00	0.00	0.10
1.4	2.00	9.52	708	800	23.5	64.5	28.0	4.22	0.92	1.07	0.09	0.37	0.14	0.44	0.00	0.08	0.12
1.5	10.00	9.52	708	800	4.52	65.3	32.4	1.01	0.30	0.20	0.03	0.03	0.03	0.02	0.00	0.02	0.01

Run #	TOS hr.	WHSV hr.$^{-1}$	Temp. K	P psig	X%	H_2	CO	*Kw	Kw	CO_2	CH_4	C_2H_4	C_2H_6	C_3H_6	C_3H_8	C_4H_{10}	CH_3OH	DME
										Carbon Yield (percent)								
1.1	0.5	9.52	708	800	15.3	8.28	7.16			51.7	25.2	0.00	12.6	0.52	7.28			2.75
1.2	1.00	9.52	708	800	18.9	8.28	8.23			50.6	20.1	0.92	11.1	1.29	12.0			3.98
1.3	1.50	9.52	708	800	20.9	8.28	9.24			49.2	15.1	1.72	9.31	3.09	16.5			5.14
1.4	2.00	9.52	708	800	23.5	8.28	10.6			49.0	12.5	2.17	8.61	4.90	15.4	0.92	0.77	5.36
1.5	10.00	9.52	708	800	4.52	8.28	6.78			65.7	12.9	3.43	4.52	5.55	4.30	1.44	0.58	1.59

TABLE 3 Continued.

Data : 8-23-'80

Catalyst : Cat. 1

Feed : CO:H₂ (33.78 : 66.22)

History : Regenerated at 773 K for 24 hr., Air Flow Rate=2cc/min.

Product Composition (mole percent)

Run #	TOS hr.	WHSV hr.$^{-1}$	Temp. K	P psig	X%	H_2	CO	CO_2	H_2O	CH_4	C_2H_4	C_2H_6	C_3H_6	C_3H_8	C_4H_{10}	CH_3OH	DME
1.6	0.25	9.52	713	750	14.4	57.7	36.5	3.16	0.83	0.69	0.02	0.40	0.01	0.04	0.0U	0.05	0.61
1.7	1.00	9.52	715	700	12.4	62.4	33.1	2.34	0.71	0.63	0.02	0.20	0.02	0.08	0.02	0.16	0.36
1.8	6.00	9.52	679	700	9.36	66.0	31.0	1.58	0.31	0.75	0.0U	0.16	0.0U	0.0/	0.0U	0.06	0.13

Carbon Yield (percent)

Run #	TOS hr.	WHSV hr.$^{-1}$	Temp. K	P psig	X%	*Kw	Kw	CO_2		CH_4	C_2H_4	C_2H_6	C_3H_6	C_3H_8	C_4H_{10}	CH_3OH	DME
1.6	0.25	9.52	713	750	14.4	7.92	6.03	51.5		11.3	0.68	12.9	0.76	1.75	0.53	0.90	19.7
1.7	1.00	9.52	715	700	12.4	7.80	6.25	50.0		13.4	0.93	8.67	1.29	4.92	1.76	3.34	15.6
1.8	6.00	9.52	679	700	9.36	10.9	9.83	49.7		23.4	0.00	10.0	0.00	6.70	0.00	1.80	8.31

TABLE 3 Continued.

Data : 9-26-'80

Catalyst : Cat. 2

Feed : CO:H$_2$ (33.78 : 66.22)

History : Fresh

Product Composition (mole percent)

Run #	TOS hr.	WHSV$_1$ hr.	Temp. K	P psig	X%	H$_2$	CO	CO$_2$	H$_2$O	CH$_4$	C$_2$H$_4$	C$_2$H$_6$	C$_3$H$_6$	C$_3$H$_8$	C$_4$H$_{10}$	CH$_3$OH	DME
2.1	3.30	1.84	623	800	6.55	66.4	31.7	0.93	0.10	0.36	0.01	0.07	0.01	0.01	0.00	0.10	0.30
2.2	3.53	1.84	640	800	14.6	67.9	27.8	1.86	0.27	1.22	0.01	0.16	0.01	0.03	0.01	0.15	0.52
2.3	4.00	1.84	633	800	11.1	68.9	28.1	1.58	0.21	0.45	0.01	0.12	0.01	0.03	0.00	0.14	0.49
2.4	6.40	1.84	611	800	5.29	68.8	29.8	0.63	0.05	0.10	0.01	0.03	0.004	0.004	0.00	0.09	0.30

Run #	TOS hr.	WHSV$_1$ hr.	Temp. K	P psig	X%	*Kw H$_2$	Kw CO	CO$_2$	Carbon Yield (percent)							
2.1	3.30	1.84	623	800	6.55	20.1	19.7	41.7	16.2	0.94	6.46	1.43	1.66	0.00	4.64	27.0
2.2	3.53	1.84	640	800	14.6	17.5	16.6	39.1	25.7	0.44	6.63	0.62	1.98	0.52	3.19	21.0
2.3	4.00	1.84	633	800	11.1	19.2	18.6	45.1	12.9	0.60	6.90	0.62	2.16	0.00	3.91	27.8
2.4	6.40	1.84	611	800	5.29	23.3	22.8	37.9	6.16	0.84	3.24	0.70	0.73	0.00	5.35	45.1

TABLE 3 Continued,

Data   : 10-28-'80

Catalyst : Cat. 3

Feed   : CO:H₂ (33.78 : 66.22)

History : Fresh

Product Composition (mole percent)

Run #	TOS hr.	WHSV hr.⁻¹	Temp. K	P psig	X%	H₂	CO	CO₂	H₂O	CH₄	C₂H₄	C₂H₆	C₃H₆	C₃H₈	C₄H₁₀	CH₃OH	DME
3.1	0.20	5.96	615	880	52.7	48.6	26.3	11.2	2.36	6.23	0.01	2.80	0.31	0.62	0.36	0.37	0.83
3.2	0.50	5.96	698	880	49.9	49.5	26.8	10.4	2.02	6.36	0.01	2.55	0.005	0.71	0.21	0.75	0.55
3.3	0.75	5.96	701	865	47.2	51.2	27.3	9.54	1.97	5.33	0.01	2.61	0.01	0.83	0.04	0.58	0.51
3.4	1.15	5.96	703	860	51.4	48.4	26.1	10.7	2.32	8.08	0.01	2.17	0.01	0.73	0.04	0.64	0.74
3.5	1.50	5.96	704	860	26.9	58.7	30.1	4.83	0.95	4.49	0.01	0.41	0.01	0.14	0.03	0.11	0.13
3.6	9.50	5.96	703	840	54.6	48.1	25.2	11.5	2.47	7.44	0.01	3.12	0.25	0.44	0.16	0.30	1.00

Carbon Yield (percent)

Run #	TOS hr.	WHSV hr.⁻¹	Temp. K	P psig	X%	*Kw	Kw	CO₂	CH₄	C₂H₄	C₂H₆	C₃H₆	C₃H₈	C₄H₁₀	CH₃OH	DME
3.1	2.20	5.96	615	880	52.7	9.32	8.76	38.2	21.3	0.08	19.1	3.22	6.33	4.87	1.28	5.61
3.2	0.50	5.96	698	880	49.9	9.08	9.52	39.2	23.7	0.20	19.1	0.05	7.91	3.22	2.78	4.11
3.3	0.75	5.96	701	865	47.2	8.80	9.08	39.1	21.9	0.10	21.4	0.13	10.2	0.74	2.39	4.15
3.4	1.15	5.96	703	860	51.4	8.67	8.57	38.8	29.2	0.10	15.7	0.12	7.93	0.58	2.30	5.31
3.5	1.50	5.96	704	860	26.9	8.58	9.89	43.6	40.5	0.24	7.31	0.28	3.70	0.99	0.98	2.42
3.6	9.50	5.96	703	840	54.6	8.67	8.92	38.1	24.6	0.07	20.6	2.47	4.36	2.12	1.00	6.60

TABLE 3 Continued.

Data : 10-31-'80

Catalyst : Cat. 3

Feed : CO:H₂ (33.78 : 66.22)

History : Regenerated at 853 K, for 24 hr., air flow at 2cc/min.

Product Composition (mole percent)

Run #	TOS hr.	WHSV₁ hr.	Temp. K	P psig	X%	H_2	CO	CO_2	H_2O	CH_4	C_2H_4	C_2H_6	C_3H_6	C_3H_8	C_4H_{10}	CH_3OH	DME
3.7	3.05	2.98	688	880	11.4	62.6	33.4	1.82	0.37	1.39	0.00	0.27	0.00	0.12	0.04	0.01	0.00
3.8	4.50	2.98	694	900	12.8	62.5	33.0	2.02	0.40	1.60	0.01	0.32	0.00	0.13	0.05	0.01	0.00
3.9	5.00	2.98	698	900	14.1	62.2	32.7	2.19	0.46	1.84	0.01	0.37	0.002	0.14	0.04	0.01	0.00
3.11	7.20	2.98	731	850	21.1	60.4	31.3	3.33	1.00	3.11	0.01	0.62	.0004	0.20	0.02	0.02	0.00
3.12	8.02	2.98	724	800	18.2	60.7	32.3	2.93	0.78	2.56	0.01	0.56	.0022	0.16	0.02	0.01	0.00

Carbon Yield (percent)

Run #	TOS hr.	WHSV₁ hr.	Temp. K	P psig	X%	*Kw H_2	Kw CO	CO_2	H_2O	CH_4	C_2H_4	C_2H_6	C_3H_6	C_3H_8	C_4H_{10}	CH_3OH	DME
3.7	3.05	2.98	688	880	11.4	9.98	9.09	42.4		32.5	0.00	12.7	0.00	8.10	4.25	0.12	0.00
3.8	4.50	2.98	694	900	12.8	9.42	9.57	41.6		32.9	0.32	13.1	0.00	8.15	3.81	0.13	0.00
3.9	5.00	2.98	698	900	14.1	9.13	9.09	40.7		34.1	0.30	13.6	0.12	7.85	3.11	0.18	0.00
3.11	7.20	2098	731	850	21.1	6.75	6.69	39.7		37.1	0.17	14.8	0.02	7.12	0.94	0.18	0.00
3.12	8.02	2.98	724	800	18.2	7.12	7.18	40.7		35.7	0.20	15.6	0.09	6.63	1.02	0.10	0.00

TABLE 3 Continued,

Data : 1-8-'81

Catalyst : Cat. 4

Feed : $CO:H_2$ (33.78 : 66.22)

History : Fresh

Product Composition (mole percent)

Run #	TOS hr.	WHSV hr.$^{-1}$	Temp. K	P psig	X%	H_2	CO	CO_2	H_2O	CH_4	C_2H_4	C_2H_6	C_3H_6	C_3H_8	C_4H_{10}	CH_3OH	DME
4.1	1.50	0.72	638	520	16.6	61.9	32.4	2.83	0.32	1.81	0.01	0.37	0.04	0.17	0.07	0.05	0.03
4.2	2.00	2.15	638	650	18.4	61.6	32.2	2.82	0.32	1.80	0.02	0.61	0.09	0.20	0.08	0.12	0.05

						%Kw	Kw		Carbon Yield (percent)								
4.1	1.50	0.72	638	520	16.6	17.0	15.9	44.0	28.1	0.40	12.0	1.68	8.11	4.08	0.80	0.93
4.2	2.00	2.15	638	650	18.4	17.0	17.0	38.6	24.7	0.66	16.8	3.61	8.16	4.33	1.70	1.35

TABLE 3 Continued

Data : 1-12-'81

Catalyst : Cat. 4

Feed : $CO:CO_2:H_2$ (20.04 : 40.70 : 39.30)

History : Under N_2 since Run # 4.2

Product Composition (mole percent)

Run #	TOS hr.	WHSV hr.$^{-1}$	Temp. K	P psig	*X%	H_2	CO	CO_2	H_2O	CH_4	C_2H_4	C_2H_6	C_3H_6	C_3H_8	C_4H_{10}	CH_3OH	DME
4.3	0.03	1.62	583	550	0.14	35.5	24.5	39.7	0.21	0.09	0.00	0.00	0.00	0.00	0.00	0.00	0.00
4.4	0.50	1.62	591	560	0.01	38.2	23.1	38.5	0.15	0.04	0.00	0.00	0.00	0.00	0.00	0.00	0.00
4.4	1.00	0.81	623	760	0.14	44.6	21.0	34.1	0.18	0.07	0.00	0.00	0.00	0.00	0.00	0.00	0.00

*X% = Total Carbon Conversion Percent

Data : 1-13-'81

Catalyst : Cat. 4

Feed : $CO:CO_2:H_2$ (20.04 : 40.07 : 39.30)

History : Regenerated at 884 K for 15 hr., air flow rate = 2cc/min.

Product Composition (mole percent)

Run #	TOS hr.	WHSV hr.$^{-1}$	Temp. K	P psig	*X%	H_2	CO	CO_2	H_2O	CH_4	C_2H_4	C_2H_6	C_3H_6	C_3H_8	C_4H_{10}	CH_3OH	DME
4.5	0.08	1.62	648	600	0.40	35.8	21.7	42.0	0.34	0.14	0.00	0.00	0.00	0.00	0.00	0.00	0.00

TABLE 3 Continued

Data   : 1-15-'81

Catalyst : Cat. 4

Feed   : CO:H2 (45.05 : 54.95)

History   : Under N_2 since Run # 4.5

Product Composition (mole percent)

Run #	TOS hr.	WHSV hr.-1	Temp. K	P psig	X%	H_2	CO	CO_2	H_2O	CH_4	C_2H_4	C_2H_6	C_3H_6	C_3H_8	C_4H_{10}	CH_3OH	DME
4.6	0.15	0.91	659	600	15.8	46.0	47.1	2.88	0.21	2.55	0.05	0.61	0.14	0.29	0.18	0.00	0.37
4.7	1.00	0.46	647	640	26.5	46.9	40.2	8.56	0.65	2.18	0.06	0.67	0.05	0.36	0.22	0.00	0.08

Carbon Yield (percent)

Run #	TOS hr.	WHSV hr.-1	Temp. K	P psig	X%	*KW	KW	CO_2		CH_4	C_2H_4	C_2H_6	C_3H_6	C_3H_8	C_4H_{10}	CH_3OH	DME
4.6	0.15	0.91	659	600	15.8	13.4	13.7	32.6		28.8	1.02	13.8	4.89	9.84	8.11	0.00	0.83
4.7	1.00	0.46	647	640	26.5	15.2	15.4	59.1		15.0	0.77	9.30	1.09	7.43	6.14	0.00	1.12

TABLE 3 Continued,

Data : 1-21-'81

Catalyst : Cat. 5

Feed : CO:H₂ (45.05 : 54.95)

History : Fresh

Product Composition (mole percent)

Run #	TOS hr.	WHSV hr.⁻¹	Temp. K	P psig	X%	H_2	CO	CO_2	H_2O	CH_4	C_2H_4	C_2H_6	C_3H_6	C_3H_8	C_4H_{10}	CH_3OH	DME
5.1	1.00	5.08	595	620	2.69	50.9	47.3	0.70	0.74	0.19	0.01	0.07	0.02	0.03	0.02	0.00	0.00
5.2	1.66	5.08	645	600	35.6	41.5	40.5	10.3	0.70	3.76	0.06	1.64	0.11	0.95	0.39	0.12	0.05
5.3	3.50	5.08	665	400	9.48	49.6	46.2	2.30	0.21	0.10	0.06	0.30	0.03	0.16	0.06	0.00	0.02
5.4	5.00	5.08	676	470	36.2	41.7	38.9	10.4	1.01	5.37	0.06	1.54	0.30	0.54	0.15	0.00	.003
5.5	5.50	5.08	707	520	56.9	37.1	28.7	17.9	2.71	9.35	0.10	2.51	0.36	0.99	0.33	0.00	0.00

Carbon Yield (percent)

Run #	*Kw	Kw	CO_2	CH_4	C_2H_4	C_2H_6	C_3H_6	C_3H_8	C_4H_{10}	CH_3OH	DME
5.1	28.5	1.01	53.4	14.8	1.98	10.3	4.07	6.92	7.19	1.40	0.00
5.2	15.6	15.3	45.9	16.8	0.58	14.7	1.50	12.7	6.87	0.52	0.46
5.3	12.6	11.6	47.6	20.5	2.43	12.4	1.70	9.65	4.64	0.00	1.03
5.4	11.3	11.0	47.1	24.3	0.53	13.9	4.05	7.33	2.80	0.00	0.03
5.5	8.36	8.54	47.2	24.7	0.51	13.3	2.86	7.87	3.59	0.00	0.21

TABLE 3 Continued.

Data : 1-27-'81

Catalyst : Cat. 6

Feed : CO:H₂ (31.75 : 68.25)

History : Reduced at 623 K for 2 hr., Hydrogen flow rate = 2cc/min.

Product Composition (mole percent)

Run #	TOS hr.	WHSV hr.⁻¹	Temp. K	P psig	X%	H₂	CO	CO₂	H₂O	CH₄	C₂H₄	C₂H₆	C₃H₆	C₃H₈	C₄H₁₀	CH₃OH	DME
6.1	1.33	0.70	680	1000	44.4	63.4	21.6	7.72	1.16	3.72	0.00	0.87	0.00	0.40	0.30	0.00	0.82
6.2	2.67	0.70	624	1000	49.7	60.5	21.0	8.79	1.31	5.21	0.00	0.89	0.00	0.45	0.16	0.47	1.28
6.3	3.01	0.70	657	1000	55.0	58.9	19.4	9.39	2.08	6.50	0.00	0.35	0.00	0.66	0.20	0.74	0.79
6.4	3.30	0.70	691	1000	70.9	52.5	13.7	12.9	5.13	11.9	0.00	2.28	0.00	1.21	0.08	0.11	0.08
6.5	3.70	0.70	715	1000	71.5	44.7	16.0	14.1	5.00	15.7	0.00	2.74	0.00	1.45	0.10	0.10	0.06

Carbon Yield (percent)

Run #	TOS hr.	WHSV hr.⁻¹	Temp. K	P psig	X%	H₂ *Kw	CO Kw	CO₂	CH₄	C₂H₄	C₂H₆	C₃H₆	C₃H₈	C₄H₁₀	CH₃OH	DME
6.1	1.33	0.70	680	1000	44.4	20.8	19.6	44.9	21.6	0.00	10.1	0.00	6.95	6.90	0.00	9.53
6.2	2.67	0.70	624	1000	49.7	20.0	19.4	42.4	25.1	0.00	8.61	0.00	6.17	3.11	2.29	12.3
6.3	3.01	0.70	657	1000	55.0	13.7	13.6	39.6	27.4	0.00	11.4	0.00	8.37	3.37	3.12	6.70
6.4	3.30	0.70	691	1000	70.9	9.67	9.63	38.5	35.4	0.00	13.6	0.00	10.8	0.95	0.33	0.45
6.5	3.70	0.70	715	1000	71.5	7.80	7.87	35.1	38.9	0.00	13.6	0.00	10.8	0.99	0.25	0.30

TABLE 3 Continued,

Data   : 1-30-'81

Catalyst : Cat. 6

Feed   : CO:CO$_2$:H$_2$ (31.69 : 0.16 : 68.14)

History : Under N$_2$ since Run # 6.5

Product Composition (mole percent)

Run #	TOS hr.	WHSV hr.$^{-1}$	Temp. K	P psig	*Xt[1]	H$_2$	CO	CO$_2$	H$_2$O	CH$_4$	C$_2$H$_4$	C$_2$H$_6$	C$_3$H$_6$	C$_3$H$_8$	C$_4$H$_{10}$	CH$_3$OH	DMK
6.6	0.25	0.69	637	1000	38.4	69.6	19.4	4.61	1.06	3.78	0.00	0.92	0.00	0.46	0.14	0.00	0.03
6.7	1.00	0.69	691	1000	80.5	60.6	6.55	10.0	10.2	9.36	0.00	2.04	0.00	0.92	0.27	0.00	0.01
6.8	1.50	1.40	693	1000	79.3	49.8	10.2	14.5	7.27	13.9	0.00	2.74	0.00	1.25	0.37	0.00	.003

Carbon Yield (percent)[2]

Run #	TOS hr.	WHSV hr.$^{-1}$	Temp. K	P psig	*Xw	Rw	CO	CO$_2$	CH$_4$	C$_2$H$_4$	C$_2$H$_6$	C$_3$H$_6$	C$_3$H$_8$	C$_4$H$_{10}$	CH$_3$OH	DMK
6.6	0.25	0.69	637	1000	38.4	16.0	15.6	35.5	30.2	0.00	14.8	0.00	11.0	4.51	0.00	0.50
6.7	1.00	0.69	691	1000	80.5	9.72	9.06	36.2	34.5	0.00	15.1	0.00	10.1	3.95	0.00	0.08
6.8	1.50	1.40	693	1000	79.3	9.57	9.79	36.7	35.8	0.00	14.1	0.00	9.66	3.80	0.00	0.02

(1) X% = Carbon Monoxide Conversion

(2) Carbon Yield from Carbon Monoxide

TABLE 3 Continued,

Data   : 2-1-'81

Catalyst : Cat. 6·

Feed   : $CH_2=CH_2$

History   : Under N_2 since Run # 6.8

Run # 6.9

Temperature=607 K

WHSV=1.87 hr^{-1}

Total $CH_2=CH_2$ Conversion

2.7%

Run # 6.11

Temperature=649 K

WHSV=1.87^{-1}

Total $CH_2=CH_2$ Conversion

13.1%

Products

H_2

CH_4

CH_3-CH_3

$CH_3-CH=CH_2$

Iso-(C_4H_{10}, C_5H_{12})

N-(C_4H_{10}, C_5H_{12})

TABLE 3 Continued,

Data   : 2-2-'81

Catalyst : Cat. 6

Feed   : $CH_2=CH_2$: H_2 (24.14 : 75.86)

History   : Under N_2 since Run # 6.11

Run #	Temp.(K)	P(psig)	WHSV(hr.$^{-1}$)	X%	S%
6.12	701	620	1.10	88.3	88.4
6.13	687	500	0.97	97.1	88.8
6.14	684	580	0.55	96.0	90.2
6.15	672	500	0.55	99.3	90.8

X% = $CH_2=CH_2$ Conversion

S% = CH_3-CH_3 Selectivity

TABLE 3 Continued,

Data : 2-3-'81

Catalyst : Ammonium and Rare Earth Exchanged Zeolon-500

Feed : $CH_2=CH_2$

History : Fresh

Run #	Temp.(K)	P(psig)	WHSV(hr.$^{-1}$)	X%
Z1	701	400	0.14	16.4
Z2	699	400	0.14	16.7

$X\% = CH_2=CH_2$ Conversion

TABLE 3 Continued,

Data   :   2-3-'81

Catalyst :   Ammonium and Rare Earth Exchanged Zeolon-500

Feed   : $CH_2=CH_2$: H_2 (35.1 : 64.9)

History :   Under N_2 since Run # Z2

Run #	Temp.(K)	P(psig)	WHSV(hr.$^{-1}$)	X%
Z3	677	580	0.055	19.5
Z4	665	580	0.055	23.9
Z5	691	550	0.055	54.2

Product Distribution (mole %)

Run #	C_2H_6	C_3H_6	C_3H_8	C_4H_{10}	C_5^+
Z3	43.0	19.6	8.98	17.0	Balance
Z4	58.3	10.6	4.78	15.1	Balance
Z5	50.6	11.6	109	18.0	Balance

X% = $CH_2=CH_2$ Conversion

TABLE 3 Continued,

Data   : 2-6-'81

Catalyst : Ammonium and Rare Earth Exachanged Zeolon-500

Feed   : $CH_2=CH_2$: H_2 : H_2O (23.6:43.6:32.9)

History   : Under N_2 since Run # 25

Run #	Temp.(K)	P(psig)	WHSV(hr.$^{-1}$)	X%
26	653	300	0.098	0.63
27	680	300	0.098	1.96

X% = $CH_2=CH_2$ Conversion

APPENDIX B

Raw Material Used in Catalyst Preparation

1. Commercial Methanol Synthesis Catalyst,
   Zinc Chromite, (Zn-0312, T 1/4, batch 69)
   The Harshaw Chemical Company.

2. Rare Earth Exchanged Erionite Powder,
   Type 41-100, Lot# 2322-2
   Union Carbide Corporation.

3. Ammonium and Rare Earth Chloride Exchanged
   Erionite and Chabizite Mixture,
   Zeolon-500, Sample# 24956
   Norton Plastics and Synthetics Division.

4. Zinc Nitrate, $(Zn(NO_3)_2 \cdot 6H_2O)$
   Lot# 776447
   Fisher Scientific Company.

5. Coppic Nitrate, $(Cu(NO_3)_2 \cdot 3H_2O)$
   Analytical Reagent Grade,
   Mallinckrodt Company.

6. Ammonium Chloride, (NH_4Cl)
   Fisher Scientific Company.

7. Anhydrous Sodium Carbonate, (Na_2CO_3)
   Fisher Scientific Company.

9. Rare Earth Chloride Mixture,
   (wt.%, $LaCl_3$=25%, $CeCl$=47.2%, $PrCl_3$=5.9%,
   $NdCl$=19.3%, $SmCl$=1.9%, $GdCl_3$=0.7%)
   Molycorp, Inc.

APPENDIX C

CALCULATION OF PRODUCT COMPOSITION

Calculation of product composition was based on experimental peak areas from gas chromatograph. The peak areas derived from the argon gas chromatograph were used to calculate the hydrogen to carbon monoxide ratio in the product. Composition on hydrogen free basis for hydrocarbons and oxygenates was calculated from peak areas dervied from the helium gas chromatograqph. The relative response factors are given in TABLE 4. The total composition was calculated using the following procedure.

Let

N_i = Moles of Compound i in the Product.

a = Hydrogen to Carbon Monoxide Ratio in the Product.

y_i = Mole Fraction on Hydrogen Free Basis
of Compound i in the Product.

x_i = Mole Fraction of Compound i in the Product.

$*A_i$ = Peak Area of Compound i in the Argon Gas
Chromatograph.

A_i = Peak Area of Compound i in the Helium Gas
Chromatograph.

$*R_i$ = Relative Response Factor of Compound i
in the Argon Gas Chromatograph.

R_i = Relative Response Factor of Compound i
in the Helium Gas Chromatograph.

1. Calculation for a :

$$a = \frac{*A_{H_2} \; *R_{CO}}{*A_{CO} \; *R_{H_2}}$$

2. Calculation for yi :

$$yi = (Ai/Ri)/(\Sigma Ai/Ri)$$

3. Calculation for xi :

$$xi = yi/(1+ay_{CO})$$

Except for hydrogen

$$x_{H_2} = (ay_{CO})/(1+ay_{CO})$$

TABLE 4

GAS CHROMATOGRAPH RELATIVE RESPONSE FACTORS

Compound	R_i[1]	*R_i[2]
H_2	–	1.00
CO	42	0.0995
CO_2	48	
H_2O	33	
CH_4	35.7	
C_2H_4	48	
C_2H_6	51.2	
C_3H_6	64.5	
C_3H_8	64.5	
CH_3OH	55	
$(CH_3)_2O$	91	
iso-C_4H_{10}	82	
n-C_4H_{10}	85	

[1] R_i = Relative Response Factor for Helium Gas Chromatograph (Dietz, 1967).

[2] *R_i = Relative Response Factor for Argon Gas Chromatograph (Experimentally Determined).

APPENDIX D

MATERIAL BALANCE

Activity and selectivity of each ~~catalyst~~ were expressed as percent conversion of carbon monoxide and carbon distribution in the product, respectively. Percent conversion of carbon monoxide and carbon distribution were calculated from material balance around the reactor. The material balance was made by forcing closure on carbon atoms. In Run # 4.3 to 4.5 the extent of reaction was expressed as total carbon conversion.

Let

$X\%$ = Percent Conversion of Carbon Monoxide

$*X\%$ = Total Carbon Conversion Percent

ni^o = Inlet Molar Flow Rate of Compound i

ni = Outlet Molar Flow Rate of Compound i

n_T^o = Total Inlet Molar Flow Rate

n_T = Total Outlet Molar Flow Rate

xi^o = Inlet Mole Fraction of Compound i

xi = Outlet Mole Fraction of Compound i

CYi = Carbon Yield of Compound i

Ci = Carbon Number of Compound i

1 Carbon Balance

$$\sum n_i{}^o C_i = \sum n_i C_i$$

$$\sum n_T{}^o x_i{}^o C_i = \sum n_T x_i C_i$$

$$(n_T{}^o)/(n_T) = (\sum x_i C_i)/(\sum x_i{}^o C_i)$$

2 Calculation of X%

$$X\% = (n_{CO}{}^o - n_{CO})/n_{CO}{}^o$$

$$X\% = [\ 1 - (n_T x_{CO})/(n_T{}^o x_{CO}{}^o)\ ]$$

3 Calculation of *X%

$$*X\% = \{(x_i C_{i\ product})/[(n_T{}^o/n_T)(x_i C_{i\ reactant})]\}$$

4. Calculation of CYi

$$CY_i = (n_i C_i)/(n_{CO}{}^o - n_{CO})$$

$$CY_i = (n_T x_i C_i)/[(n_T{}^o/n_T)(x_{CO}{}^o) - x_{CO}]$$

APPENDIX E

EQUILIBRIUM CONSTANT OF WATER GAS SHIFT REACTION

Water Gas Shift Reaction

$$CO + H_2O \longrightarrow CO_2 + H_2$$

Theoretical Equilibrium Constant Value

$$*Kw = \exp[(5639.5/T) + 1.077\ln T + 5.44 \times 10^{-4}T -$$
$$1.125 \times 10^{-7}T^2 - (49170/T^2) - 13.148]$$

T = Reaction Temperature (K)

Experimental Equilibrium Constant Value

$$Kw = (x_{CO_2} \, x_{H_2})/(x_{CO} \, x_{H_2O})$$

xi = Mole Fraction of Compound i in Reaction Effluent

VITA

Mr. Ting Yee Chan was born to Mr. and Mrs. Suey Chin in Hong Kong and was immigrated with his family to United States in 1968. He received his primary and secondary schooling at Hong Kong and Houston, Texas, respectively. He obtained his Bachelor of Science degrees in Chemical Engineering and Chemistry from Massachusetts Institute of Technology in 1979.

Mr. Chan's permanent address is

7810 Clarewood
Houston, Texas 77036

This Thesis was typed by the author.